

Review

The Detection of GRBs at VHE: A Challenge Lasting for More than Two Decades, What is Next?

Alessio Berti ^{1,*}  and Alessandro Carosi ^{2,*} ¹ Max-Planck-Institut für Physik, D-80805 Munich, Germany² INAF-Osservatorio Astronomico di Roma, I-00136 Rome, Italy

* Correspondence: aberti@mpp.mpg.de (A.B.); alessandro.carosi@inaf.it (A.C.)

† These authors contributed equally to this work.

Abstract: Unveiling the mystery of gamma-ray bursts (GRBs) has been the target of many multi-wavelength observational and theoretical efforts during the last decades. The results collected by current and past space-based instruments have provided important insights into the mechanisms at the origin of their prompt and afterglow phases. On the other hand, many questions, such as the the origin of the multi-GeV signal observed in a large number of events, remained unanswered. Within this framework, the first firm detections of a very-high-energy (VHE, $E \gtrsim 100$ GeV) emission component by MAGIC and H.E.S.S. collaborations represented an important, long-awaited result for the VHE astrophysics community. However, while such discoveries opened a new era in the study of GRBs, they also provided an unexpected complexity due to the differences between the phenomenology of the observed events. This revealed that we still have an incomplete comprehension of GRB physics. In the nearby future, observations by the Cherenkov Telescope Array Observatory (CTAO), with unprecedented sensitivity in the VHE band, will have a key role in the study of these enigmatic objects and their interactions with the surrounding environment. In this review we will cover the recent GRB history, highlighting the efforts of follow-up campaigns by the VHE community that led to the first VHE GRB detection, and outlining what we can expect from future facilities in the next decades.



Citation: Berti, A.; Carosi, A. The Detection of GRBs at VHE: A Challenge Lasting for More than Two Decades, What is Next? *Galaxies* **2022**, *10*, 67. <https://doi.org/10.3390/galaxies10030067>

Academic Editors: Elena Moretti, Francesco Longo and Yi-Zhong Fan

Received: 10 March 2022

Accepted: 18 April 2022

Published: 10 May 2022

Publisher's Note: MDPI stays neutral with regard to jurisdictional claims in published maps and institutional affiliations.



Copyright: © 2022 by the authors. Licensee MDPI, Basel, Switzerland. This article is an open access article distributed under the terms and conditions of the Creative Commons Attribution (CC BY) license (<https://creativecommons.org/licenses/by/4.0/>).

Keywords: gamma-ray bursts; very high energy; IACTs

1. Introduction

In 2019, the announcement of the first detection of VHE gamma-ray emission from GRB 180720B [1], GRB 190114C [2], and GRB 190829A [3] represented a long-awaited result for the astrophysical community and the end of a quest lasting for more than twenty years. The detection of a VHE counterpart of GRBs always posed a major challenge for imaging atmospheric Cherenkov telescopes (IACTs) from both the technical and the scientific point of view see, e.g., [4,5]. On the other hand, catching such a signal has a crucial impact on understanding the poorly-known physics of these objects during the different phases of their emission, motivating the continuous efforts in the VHE observational window. In fact, the observed radiation still has an uncertain origin in many aspects. According to the widely accepted relativistic shock model originally proposed in [6], GRB emission arises from the conversion of the kinetic energy of a relativistic outflow into electromagnetic emission. The details of this conversion remain poorly understood. However, the dissipation might happen in the form of collisionless shocks between the relativistic flow itself (internal shocks, responsible for the prompt phase) or with the circumburst medium (external shocks, responsible for the afterglow emission phase). Alternatively, other dissipation mechanisms have been considered in literature and, noticeably, the possibility of having magnetic reconnection events as the base for particle acceleration; see, e.g., [7,8]. The nature of the possible radiative processes at work is also not firmly established yet. Particles inside the outflow and accelerated towards relativistic regime can emit the observed high-energy photons via many possible non-thermal mechanisms, in particular during the early

afterglow phase. In this regard, the prompt-to-early-afterglow phase still remains the least understood in GRB dynamics. Prompt emission spectra have been largely fitted through the so-called Band function [9], an empirical function composed by two smoothly connected power-law functions at a specific break energy. While historically the band function worked quite well in fitting prompt spectra in the 10 keV–1 MeV range for many GRBs, more recent works have showed that extra emission components in the form of an additional power-law and/or a photospheric blackbody component are needed to better fit the observed emission both at lower and at higher energies with respect to the GRB peak energy (see, e.g., [10,11] and references therein). Such components might account for a revision of the theoretical interpretation of the observed radiation as possible synchrotron emission from electrons accelerated within the relativistic outflow. Synchrotron emission has been shown to be in tension with experimental data in many events; see, e.g., [12,13]. Nevertheless, synchrotron is believed to play an essential role in GRB physics and it has been largely considered as the most natural process to explain the GRB sub-MeV emission both during the prompt and afterglow; see, e.g., [14–16]. Furthermore, it has also been suggested that the high-energy photons above ~ 10 MeV observed by the *Fermi*-LAT (Large Area Telescope) [17], and extending after the end of the prompt emission, might be generated by synchrotron radiation produced in external shocks [18]. However, the observation of an emission component at VHE, as recently detected by current IACTs, challenges the synchrotron-alone emission models and, ultimately, the particle acceleration mechanisms at work in GRBs. In internal/external relativistic shock models, particles can be accelerated up to a maximum Lorentz factor achieved when the comoving acceleration time matches the typical radiative cooling time. The corresponding maximum photon's energy emitted by a synchrotron is around ~ 50 MeV in the comoving frame corresponding to an observed $E_{max} \sim 50 \text{ MeV} \times \Gamma / (1 + z)$ (synchrotron burnoff limit), where Γ is the bulk Lorentz factor of the relativistic outflow and z is the redshift of the source. In the case of GRBs, arguments for the hypothesis of an emitting region moving towards the observer with a bulk Lorentz factor $\Gamma \sim \text{few} \times 100$ are known and used to solve inconsistencies between the observed non-thermal emission above the pair production threshold ($\gamma\gamma \rightarrow e^+e^-$) and the time variability observed during the prompt phase; see, e.g., [19]. With the *Fermi* satellite, some firm estimations for Γ have been achieved using the maximum photon's energy detected by *Fermi*-LAT in the GeV band. For some particularly bright GRBs, values exceeding $\approx 10^3$, as in the case of $\Gamma \sim 900$ for GRB 080916C [20] and $\Gamma \sim 1200$ for GRB 090510 [21], have been measured. Although those values dramatically differ from any other relativistic motion observed in other astrophysical sources, they would still appear moderate if considering the signal caught by IACT in the hundreds of GeV or even TeV band. Furthermore, after the end of the prompt phase, Γ decreases with time [22], implying that the maximum energy achievable by synchrotron photons decreases as well. Thus, HE and VHE signals detected deeper in the afterglow phase, such as in the case of GRB 190829A, abundantly exceed the synchrotron burnoff limit, challenging the simple shock acceleration/synchrotron model. The complexity of scenarios provided by the latest IACT results shows a still unsatisfactory level of comprehension of GRB physics and the importance of continuing the observation of GRBs in the VHE band with next-generation IACTs. In the coming decades, the premier facility for VHE astrophysics will be the CTA observatory that will perform observations in the >10 GeV range with unprecedented photon statistics and sensitivity, allowing to investigate the parameter space of a wide range of VHE-transient emitters and their characteristics.

In this paper, we will revise the main experimental results that historically helped in shedding light into the GRB physics in the HE (high energy, $E \gtrsim 100$ MeV) and VHE domains. The paper is organized as follows: in Section 2 we briefly introduce the theoretical emission models used to interpret GRB HE and VHE emission. In Sections 3 and 4 we will summarize the main experimental steps that brought us to the detection of GRBs in the HE and VHE band. Section 5 investigates the open issues that still affect the characterization

of GRBs at VHE and that will hopefully be solved by next-generation instruments finally described in Section 6.

2. Models for HE and VHE Emission in GRBs

Although not within the primary scope of this paper, it is important to briefly summarize the main interpretative models able to explain the emission at the highest energies. Many theoretical models were proposed in the last decades to explain the emission from GRBs, with predictions extending to the HE and VHE range. Usually, in these models, the origin of HE and VHE emission can take place in both internal or external shocks. In both cases, either leptonic or hadronic processes might be considered as possible explanation of the observed emission. As already mentioned in the previous section, synchrotron emission is one of the most discussed for the emissions in the keV–MeV band. At higher energy, synchrotron photons might interact through inverse Compton with ultra-relativistic electrons of the outflow. This amplifies the energy of the seed photons by a factor of γ_e^2 , where γ_e is the electron's Lorentz factor. Depending on the specific microphysical parameters of the emitting region, this synchrotron self-Compton (SSC) emission can arise and easily produce photons in the HE and VHE ranges. Detailed predictions for such a model are given in [23,24], where the suppression of inverse Compton due to the Klein–Nishina (KN) effect is also widely discussed. This effect can explain the delay observed between the keV and HE emission (see Section 3) if the KN regime is dominant at early times, but then at late times the inverse Compton enters the Thomson regime; see, e.g., [25–27]. Hadronic particles can be also shock-accelerated in the same way as leptons, influencing (potentially) the HE and VHE emission. Hadronic models comprise synchrotron emission from protons or cascade emission (synchrotron) from secondary pairs [28,29]. In the synchrotron scenario, the delay between low- and high-energy emission can be explained as the time required to accelerate protons to high enough energies. However, being a poor emitter compared to leptons, proton energy is mainly lost through p- γ interactions rather than by synchrotron. In this case, the required energy budget to achieve comparable emission level with leptonic processes is normally well above the observed ones ($\gtrsim 10^{55}$ erg), although this requirement can be relaxed with a narrow jet opening angle ($<1^\circ$). In the case of external shocks, one of the main models considered for HE and VHE emission is SSC at the (external) forward shock. In such a case, a separate component with a second peak at high energies is expected [14,15]. This model was largely used to explain the HE emission in some *Fermi*-LAT bursts (see, e.g., [30–32]), as we will describe further in the next sections. SSC is proposed to produce HE photons also in the reverse shock [33] and it was shown to explain the HE component of some GRBs [34]. Furthermore, in the external shock scenario, hadronic models are also a possible option in order to account for HE and VHE emission. However, as in the internal origin case, hadronic processes suffer the same issue on the required energetics, although a possible non-dominant contribution to the overall HE–VHE emission cannot be completely excluded [35]. We refer to [36] for a more detailed review on theoretical emission models.

3. Gamma-Ray Bursts Observations at High Energies

The first systematic and comprehensive study of GRBs population was carried out by the space-based telescope Compton Gamma-Ray Observatory (CGRO), which operated for about 9 years between April 1991 and June 2000. Thanks to its four onboard instruments and, in particular, the Burst And Transient Source Experiment (BATSE: 25 keV–2 MeV) and the Energetic Gamma-Ray Experiment Telescope (EGRET: 20 MeV–30 GeV), it was possible to have an energy coverage ranging from the soft X-rays to the HE gamma rays. This provided the first meaningful interpretation of the GRB phenomenon. Specifically, thanks to EGRET, it was possible to start studying the properties of the high-energy emission ($\gtrsim 10$ –20 MeV) of GRBs for the very first time. A notable event was detected by EGRET on 17 February 1994, GRB 940217 [37]. The burst had a duration of 180 s as measured by BATSE. Ten HE photons were detected by EGRET with energy up to ~ 3 GeV during

the prompt emission. Eight other HE photons were detected in the following ~ 600 s. After the occultation due to the Earth, EGRET registered another 10 photons more than 4700 s after the burst trigger. The highest-energy photon detected in this observation phase had an energy of 18 GeV (see Figure 1), and for many years it represented the highest energy photon ever detected from a GRB. This delay in high-energy emission was observed in other GRBs detected by EGRET, although not as evident as for GRB 940217 (see [38]). Furthermore, the detection of HE photons pointed out to the possible presence of additional spectral components overlapped to the classical sub-MeV band emission. From a different perspective, the presence of a delayed emission was also considered as an opportunity for TeV detectors, such as IACTs, that needed to be repointed for start follow-up but also for extensive air shower (EAS) arrays.

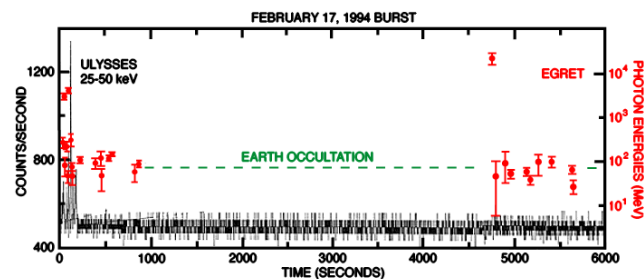


Figure 1. EGRET light curve for the GRB 940217 with the detection of an ~ 18 GeV photon that occurred about 90 min after the GRB onset. From <https://fermi.gsfc.nasa.gov/science/resources/docs/vwp/>. Available online: (accessed on 10 April 2022).

A hint of a distinct emission component in the HE range was found in the case of GRB 941017 [39]. This event showed a $\gtrsim 200$ MeV signal rising between 14 and 47 s after the T_0 and lasted for approximately 200 s in addition to the typical GRB emission which peaked at \lesssim few hundred keV. The HE component is well fitted by a power law with index close to -1 up to 200 MeV throughout all the burst duration, while the low-energy spectrum was well described by the classical band function. Data were inconsistent with a simple synchrotron model interpretation, and other theoretical emitting scenarios were considered, such as synchrotron self-Compton (SSC) from the reverse shock, created when the GRB ejecta are decelerated by the ambient medium. Additional interpretations were also considered, such as a possible hadronic origin of the HE component, as well as an HE emission taking place in external shocks [33]. Despite these earliest observations that helped significantly in determining some HE properties of GRB, the limited statistics and the large dead time typical of EGRET did not allow to measure precise spectra and study in detail the short timescale variability in the emission, especially during the prompt phase. Many questions were left unanswered after EGRET stopped operations in 2000, mostly related to the jet physics, particle acceleration, and to the nature of the high-energy emission. In this context, there were many expectations for the launch of AGILE (Astro-Rivelatore Gamma a Immagini Leggero) and *Fermi Gamma-ray Space Telescope* (*Fermi* in short). Using silicon trackers, the limitations of the old generation of gamma-ray imagers, such as the small FoV and the large dead time, were partially solved. AGILE, launched in 2007, was the first instrument with this kind of technology, followed by *Fermi* in 2008. These satellites opened a new era in the studies of GRBs in the HE band.

AGILE's onboard instrumentation includes a gamma-ray imaging detector (GRID) sensitive in the 30 MeV–50 GeV band, a hard X-ray monitor (SuperAGILE: 18–60 keV), and a mini-calorimeter (MCAL) non-imaging gamma-ray scintillation detector sensitive in the 350 keV–100 MeV energy range [40]. With the detection of GRB 080514B [41], AGILE confirmed the presence of a delayed and relatively long-lasting high-energy emission, as seen in the EGRET events. The burst was detected by all the instruments onboard AGILE: GRID detected photons from 25 MeV up to 300 MeV, while in the hard X-ray band (SuperAGILE), the 17–50 keV light curve showed a multi-peaked structure with a total

duration of 7 s. The high-energy emission did not show any correlation with these peaks, and only three photons above ~ 30 MeV were detected within 2 s from T_0 . All the other high-energy photons were recorded when the X-ray emission had already faded, up to ~ 30 s after the burst onset.

GRB 100427B [42] is another notable GRB detected by AGILE. Both the MeV and GeV light curves show two bumps where the second peak is broader than the first, with no significant delay with respect to the lower-energy emission in the X-ray band. The second bump resulted harder than the first, and spectral evolution between the bumps and the inter-bump region in MCAL data were detected at the level of 4.0σ . A single power law was shown to be adequate to model the spectrum from 500 keV to 3.5 GeV, given that the spectral index of the MCAL + GRID data and GRID data only were compatible with each other. Even if the redshift was not measured for this GRB, given the highest energy photon of 3.5 GeV, the minimum Lorentz factor during the prompt emission was constrained to be between 50 and 900. For other GRBs observed by AGILE, not detected by GRID, upper limits were derived and found to be consistent with an extrapolation of the band spectrum up to GeV energies; see [43].

Fermi was launched in 2008, approximately one year after AGILE. *Fermi* uses the same detector technology as AGILE and it was designed to be a proficient gamma-ray satellite with improved capabilities with respect to previous-generation gamma-ray detectors. The spacecraft hosts two instruments on board. The gamma-ray burst monitor (GBM) is composed of 14 scintillators (twelve sodium iodide and two bismuth germanate) and covers the energy range from a few keV to ~ 30 MeV [44]. With a field of view of almost 4π , it is devoted to the detection of GRBs or other burst-like sources and to the quick distribution of GRB localizations. The second instrument is the pair-production telescope LAT [17], operating in the energy range 20 MeV–300 GeV. The adoption of the silicon strips detector technology for the *Fermi*-LAT led to substantial improvements in terms of angular resolution and timing capabilities. Thanks to a big calorimeter, the sensitive energy range of the *Fermi*-LAT extends up to few hundreds of GeV, also providing a good energy resolution. Owing to its efficient design, *Fermi* delivered and is still delivering more detailed results and the highest statistics for studying GRBs in the HE regime. At the same time, it is providing an invaluable overlap with ground-based VHE facilities.

GRB 080825C [45] was the first GRB detected by *Fermi*-LAT, a long burst with $T_{90} = 27$ s. The highest-energy photon was a (572 ± 58) MeV photon detected at $\sim T_0 + 28$ s, just after the low-energy emission measured in *Fermi*-GBM faded almost completely. The spectrum of GRB 080825C in different time bins is well fitted by a band function with a hard-to-soft evolution of the νF_ν spectrum peak energy (E_{peak}). In the last time bin, the spectrum is well described by a power law with a harder index -1.95 ± 0.05 . This property and the low flux ratio between the first two peaks in the *Fermi*-LAT light curve may suggest a different region of origin for their emission: within the internal and external shock respectively [45].

GRB 080916C [20] is the second *Fermi*-LAT detected burst and one of the brightest in the *Fermi*-LAT GRB sample, with a measured redshift of $z = 4.35 \pm 0.15$ and a total isotropic energy release of 8.8×10^{54} erg. Compared to the signal measured in *Fermi*-GBM, this GRB showed a delayed onset of the LAT pulse and a longer-lived emission in the $\gtrsim 100$ MeV band. These features will be confirmed in other GRBs detected at HE. The comparison between the *Fermi*-GBM and the *Fermi*-LAT light curves (Figure 2) showed that the first *Fermi*-GBM peak has no corresponding peak in the *Fermi*-LAT light curve. The first *Fermi*-LAT pulse is instead temporally coincident with the second *Fermi*-GBM peak. A common origin for the two peaks but in spatially different regions is the most likely explanation, with different pairs of colliding shells within the internal shock scenario. The long-lasting emission above 100 MeV was detectable up to $T_0 + 1400$ s, well after the low energy emission faded. The time decay of the high energy flux is well fitted by a power law $t^{-\alpha}$ with $\alpha = -1.2 \pm 0.2$, a value that is typical for other *Fermi*-LAT-detected GRBs. The *Fermi*-GBM flux decays as $t^{-0.6}$ up to $T_0 + 55$ s with a steepening in the index ($\alpha \sim -3.3$) afterward. This might indicate a different nature of the high-energy emission, although no

spectral hardening is seen in the *Fermi*-LAT late spectrum, as in the case of GRB 080825C. As in other HE detected burst, GRB 080916C data were used to set a lower limit to the Lorentz factor of the blast-wave, $\Gamma_{\min} = 887 \pm 21$. Even if most of the *Fermi*-LAT-detected GRBs belong to the long class, it helped to study the high-energy emission of short GRBs as well. Among them, some interesting cases are GRB 081024B [46] and GRB 090510 [21,47].

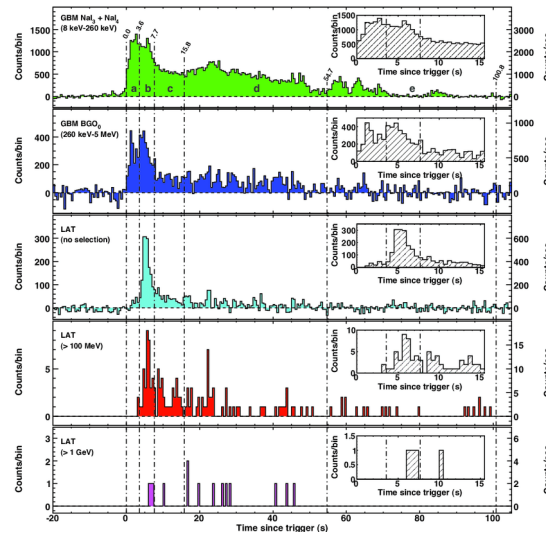


Figure 2. *Fermi*-GBM and *Fermi*-LAT combined light curve for GRB 080916C. Reprinted with permission from Ref. [20].

GRB 081024B is the first short GRB detected by *Fermi*-LAT, with a duration of 0.8 s. In addition for this GRB, the emission above 100 MeV is delayed and is long-lasting ($T_{90} = 2.6$ s above 100 MeV).

GRB 090510 is a short GRB which was detected by both AGILE and *Fermi*. Both instruments confirmed the presence of a ~ 0.1 s-delayed HE emission component after the onset measured in *Fermi*-GBM. The detection of a 30.5 GeV photon during the prompt phase allowed an evaluation of the bulk Lorentz factor that resulted in a very high lower limit of $\Gamma_{\min} \gtrsim 1200$, assuming the estimated redshift $z = 0.903$. However, the most remarkable feature of GRB 090510 is that its time-integrated spectrum for the GBM+LAT prompt emission data cannot be fitted with a simple band function. An additional power law component with index -1.62 ± 0.03 , dominant below 20 keV and above 100 MeV, is needed to describe the spectrum (see Figure 3) [21]. In the afterglow phase, a signal has been detected by *Fermi*-LAT up to $\sim T_0 + 150$ s, which prompted several theoretical interpretations for both the prompt and afterglow phases. Some of them consider synchrotron radiation as theoretical interpretation of the low-energy (band) emission while the hard extra-component is generated by the synchrotron photons Compton upscattered by the same electrons accelerated in the shock (synchrotron self-Compton); see, e.g., [48]. This scenario is commonly used to model emission in other VHE sources, such as blazars, and the SSC component results are stronger for a large ratio of non-thermal electron to magnetic-field energy density and low values of Γ . However, in the case of GRB 090510, such an interpretation has difficulties in explaining the delayed onset of the high-energy emission. For example, the SSC model predicts a too-short delay in the assumptions of weak magnetic field [21]. Hadronic scenarios were also proposed but the proton injection isotropic-equivalent energy required is more than two orders higher than the one actually measured for the burst [49]. These observations of short GRBs show that they can be as relativistic as long GRBs and that they seem to have a better efficiency in emitting gamma rays, given that the energy emitted in the high-energy (100 MeV–10 GeV) band is greater than the one at low energy (20 keV–2 MeV). However, the statistic is still limited to few bursts to draw a definitive conclusion.

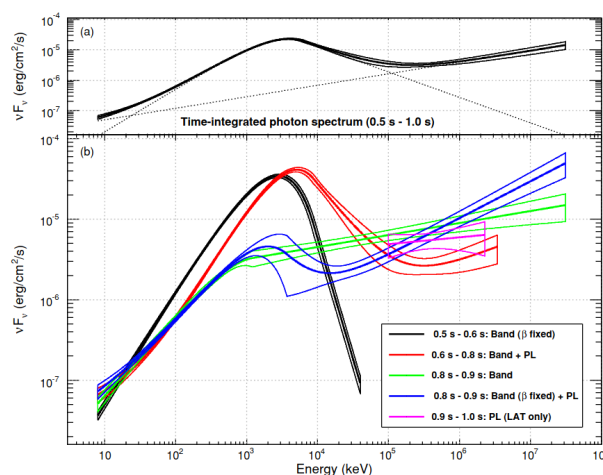


Figure 3. Time-integrated spectrum (upper panel) and model spectra (with $\pm 1\sigma$ error contours) used to fit the emission of GRB 090510 in different time bins. Reprinted with permission from Ref. [21].

As a final example, it is worth to report the *Fermi*-LAT detection of GRB 130427A, one of the most powerful GRBs observed at redshift $z = 0.34$ [50]. The event showed the highest fluence (4.2×10^{-3} erg/cm² from 10 keV to 20 MeV), the highest energy photon (95 GeV at $T_0 + 244$ s), and the longest-lasting HE emission extending up to 100 ks after the trigger. It had a total apparent isotropic gamma-ray energy release of $\sim 1.4 \times 10^{54}$ erg. The event showed a delayed emission starting about 10 s after the trigger when the *Fermi*-GBM brightest emission already ended. Therefore, the *Fermi*-LAT emission is temporally distinct from the one in *Fermi*-GBM (see, e.g., Figure 1 in [50]), and this suggests different regions or mechanisms for the two emissions. Having a 95 GeV photon in the early afterglow and a 32 GeV one at $T_0 + 34.4$ ks, it is difficult to accommodate them within the standard synchrotron emission from electrons accelerated in the external shock or in the SSC scenario, at least according to [50]. In [51], the combined X-ray, GeV, and optical data were used to fit the spectrum with a single synchrotron component while authors in [32] proposed an afterglow SSC emission to explain the long-lasting emission. These results show the puzzling interpretative scenarios of GRBs at HE and the lack of a clear physical explanation, both in the prompt and in the afterglow phases.

Summarizing, *AGILE* and *Fermi* showed that HE emission from GRBs share some common features:

1. The band model is not able to describe the joint low- and high-energy spectra. An additional component (e.g., extra power law) or a cutoff are needed, with no unique solution for all GRBs. Other GRBs may require an additional thermal blackbody component.
2. *Fermi*-LAT-detected GRBs are among the brightest detected by the *Fermi*-GBM. The energy released in high-energy gamma-rays (> 100 MeV) in the extended temporal phase is about 10% of the total energy radiated in the prompt phase.
3. The high-energy emission is delayed and longer-lasting with respect to the low-energy one. It might extend in time well after the low-energy emission has faded. The temporal decay is generally consistent with a power law behavior $t^{-\alpha_L}$ with $\alpha_L \sim 1$.

These conclusions are the same as those resulting from the first *Fermi*-LAT GRB catalog, presented in [52], an in-depth systematic study of *Fermi*-LAT-detected GRBs in the first three years of the mission.

4. GRB Observation at VHE: The Story so Far

The field of VHE transient astronomy has been rapidly evolving for the last 30 years, mainly (but not only) due to the development of the imaging atmospheric Cherenkov technique. Towards the end of the last century, the first IACT experiments were built and

started operation, proving the robustness and reliability of this detection technique through the first detection of the standard candle VHE emitter, the Crab Nebula [53]. In parallel with the confirmation of the IACT technique, GRBs science was entering for the first time in a phase of systematic population studies thanks to the BATSE and EGRET instruments on board the CGRO (see Section 3) but also to the BeppoSax satellites, launched in 1996 [54]. The latter, thanks to the contemporary presence on the same platform of both wide- and narrow-field instruments, was able to provide, for the first time, arcminute localizations of GRB positions although with \sim hours delay timescale. As reported in the previous section, the discovery of a delayed and persistent HE emission component in some of the EGRET-detected events (see, e.g., [37]) definitively pushed the search for a component also at VHE. Real-time triggers provided through the BATSE Coordinates Distribution Network (BACODINE) and the third Interplanetary Network IPN-[55], although with relative large uncertainties in the localization (\gtrsim few degrees), allowed, for the first time, the rapid follow-up by ground-based telescopes including the earliest VHE facilities, such as the first IACTs and EAS arrays. Although not presenting imaging capabilities, EAS arrays were able to cover a wide portion of sky, allowing for offline search of a coincidence signal in the ultra-high-energy (UHE) gamma-ray band (\gtrsim 100 TeV). Such a search for emission of TeV/PeV gamma rays associated with GRBs has been extensively reported in literature by many different EAS collaborations, such as CYGNUS-I [56], HEGRA-AIROBICC [57], CASA-MIA [58], and EAS-TOP [59]. None of these revealed any convincing evidence for emission in the >100 TeV band. It is important to remark that at the time of these observations, a firm determination of GRB distance was still missing and the detection of \gtrsim 100 TeV photons represented a concrete possibility and an important insight into the origin (cosmological or local) of these events. A largely discussed, although not conclusive, hint for an emission in the \sim TeV band came from the Milagrito experiment [60]. Milagrito was a TeV EAS array based on the water Cherenkov detection technique, a prototype of the larger Milagro detector. The array operated between February 1997 and May 1998 in the 500 GeV–20 TeV energy range, observing 54 BATSE GRBs localized in its field of view. A possible $\sim 3.5\sigma$ evidence of TeV emission was found in the case of GRB 970417A, likely caused by photons of \gtrsim 650 GeV [61]. This measurement could indicate the first detection of a GRB in VHE regime; however, the weakness of the signal did not allow any spectral analysis of the event. Moreover, no other similar detection was observed by the later Milagro experiment in the same energy range, making the reliability of this observation less constraining.

The first follow-ups by an IACT at lower energies compared to EAS arrays (above \sim 250 GeV), took place at the beginning of the 1990s, thanks to the Whipple 10 m reflector. These observations represented the first use of the IACT technique in exploring the GRB phenomenon complementing, although not yet overlapping, the band coverage guaranteed by the contemporaneous space-based instrumentation. Whipple reported no significant emission in the VHE band from a sample of nine GRBs observed between May 1994 and December 1995. The obtained upper limits are of the order of that expected for prompt emission if the burst emission extends to TeV energies with a band-like extrapolation without breaks or cutoff [62]. This confirmed the effectiveness of the IACT technique in proving GRB physics while pointing out some of the main difficulties of these follow-ups. Differently from EAS array, being (relatively) narrow field instruments, IACTs need to be repointed to GRB coordinates in order to start the follow-up. This introduced a delay that, for these earliest observations, ranged from 2 to 56 min. Furthermore, due to the large uncertainty in the BATSE localization of the events, the majority of the observations were performed with the source located off-axis (or in some case outside the telescope's field of view), significantly decreasing the sensitivity of the instrument and requiring multiple pointings to scan the burst region (Figure 4). The necessity of having rapid repointing and follow-up observations was the core issue in 2004 of the launch of the *Swift* satellite [63]. *Swift* operates as a multi-band satellite incorporating three different instruments: a large FoV soft-gamma detector for GRBs trigger (BAT, burst alert telescope: 15–150 keV) and

two telescopes in the X-ray (XRT, X-ray telescope: 0.3–10 keV) and UV band (UVOT, UV optical telescope) for the low-energy follow-up. These instruments were mounted on an autonomously slewing spacecraft that, using the same driven-logic of BeppoSax, made possible the observation and the precise localization of GRBs within tens of seconds from the event onset. These key features significantly improved the understanding of the early afterglow phase and its connection with the prompt emission [64]. Almost in parallel to the launch of *Swift*, the new generation of IACTs MAGIC (<https://magic.mpp.mpg.de/>), H.E.S.S. (<https://www.mpi-hd.mpg.de/hfm/HESS/>), and VERITAS (<https://veritas.sao.arizona.edu/>) (all websites accessed on 10 April 2022) started operations opening a new phase in GRB study at VHE. Some of these telescopes were explicitly designed to optimize the follow-up observation of GRBs, with the aim to reach the few tens of GeV energy threshold, bridging the observational energy gap between the space-based instrumentation and enlarging the available gamma-ray horizon, one of the critical aspects for high redshift sources such as GRBs. Extensive follow-up campaigns on GRBs were performed by all IACTs collaborations along approximately 15 years of observations and they also progressively bridged the energy coverage gap with AGILE and *Fermi*. However, these extended observations did not report any conclusive evidence of VHE emission from the observed events. We briefly summarize the main outcomes of this first decade of observation.

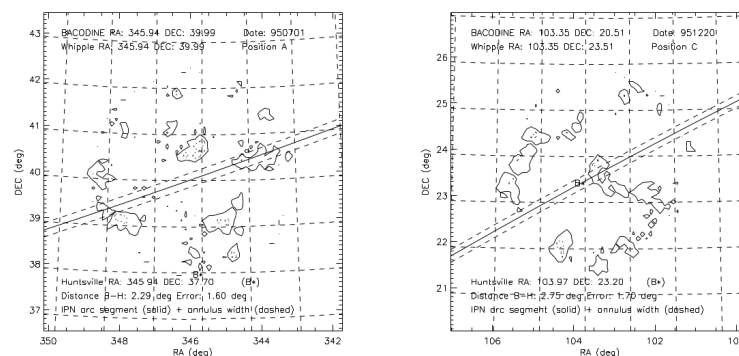


Figure 4. Excess sky map for two pointing positions during the follow-up of two GRBs by Whipple telescope in 1995. The refined position of the event is marked as B* in the plot while the IPN confidence areas are derived from BATSE and *Ulysses* data. Reprinted with permission from Ref. [62].

MAGIC (Major Atmospheric Gamma Imaging Cherenkov) is a system of two 17 m IACTs, with a $\sim 3.5^\circ$ field of view located on the Canary Island of La Palma. Observations started in 2004 with a single standalone telescope until a second one was added in 2009, improving angular resolution and sensitivity. Extensive follow-up campaigns on GRBs were performed since the beginning of the operations, taking advantage of the instruments low-energy threshold ($\lesssim 50$ GeV) combined with a very fast repositioning speed ($\sim 7^\circ/\text{s}$). Despite the continuous improvement in instrument's reaction to external GRB triggers and in data analysis along the years, no significance evidence of VHE emission was reported during the first ~ 15 years of observations. However, remarkable results were achieved in terms of performance, such as the first follow-up of GRBs during the prompt emission phase for a bunch of events such as GRB 050713A (Figure 5, left panel), GRB 131030A, GRB 141026A, and GRB 150428B [4,65–67]. Furthermore, within the framework of relativistic shock-wave models, possible emission in the VHE band by synchrotron-self-Compton mechanism in afterglow has been modeled and discussed by the MAGIC collaboration in relation to the obtained upper limits on a few interesting events such as GRB 0804030 [68] and GRB 090102 (Figure 5, right panel), one of the first GRBs with simultaneous data taken with *Fermi*-LAT [5]. Although not particularly constraining, these results showed that IACT performances were mature enough to play an important role in GRB studies.

The High-Energy Stereoscopic System (H.E.S.S.) is an array of IACTs operating in Namibia since 2004. The so-called phase-I included four 12 m diameter telescopes, with an energy threshold of ~ 100 GeV at zenith, and a 5° field of view. In 2012, a large 28 m diameter telescope was added to the array. This telescope is characterized by a faster repointing and large collection area (~ 600 m²) that guarantee an energy threshold of 50 GeV. Thus, it is a transient-oriented instrument. The introduction of the new telescope marked the beginning of the H.E.S.S. phase-II operations. Despite these improvements, also for H.E.S.S., the first 15 years of observations did not reveal any significant emission for the observed events. Collection of follow-ups and possible interpretation of the obtained upper limits are summarized in different collaboration works, such as in [69–72].

VERITAS (Very Energetic Radiation Imaging Telescope Array System) is an array of four 12 m IACTs located in Arizona operating in the $\gtrsim 100$ GeV band. The system is the successor of Whipple and has activated a GRB observing program since the beginning of the operations in 2007. VERITAS did not report any detectable VHE emission from the sample of the observed GRBs; however, in 2013, VERITAS was the only IACT able to follow up GRB 130427A, the first GRB observed at VHE (see Section 3). Unfortunately, VERITAS was only able to perform observations on GRB 130427A approximately 20 h after the event’s onset. Although at that time *Fermi*-LAT was still able to detect activity in the HE band, VERITAS did not report a significant emission in the VHE range. The achieved upper limits at ~ 100 GeV were able to significantly constrain the proposed emission model, pointing out tensions within the Klein–Nishina and Thomson emission regimes [73] (Figure 6).

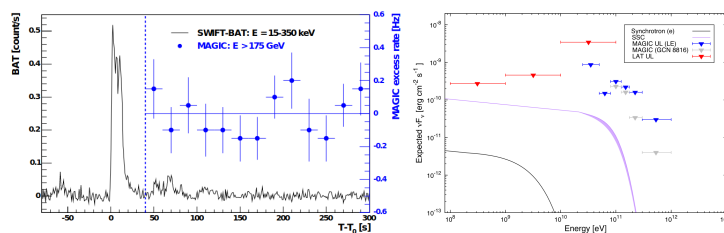


Figure 5. (Left) MAGIC excess event rate above the energy threshold of 175 GeV compared with the *Swift*-BAT light curve for GRB 050713A, the first prompt emission followed by an IACT. The vertical line shows the beginning of observations with the MAGIC telescope. Reprinted with permission from Ref. [65]. (Right) MAGIC and *Fermi*-LAT overlapping upper limits for GRB 090102. These results are compared to a leptonic synchrotron+SSC afterglow model. From model and data analysis described in [5].

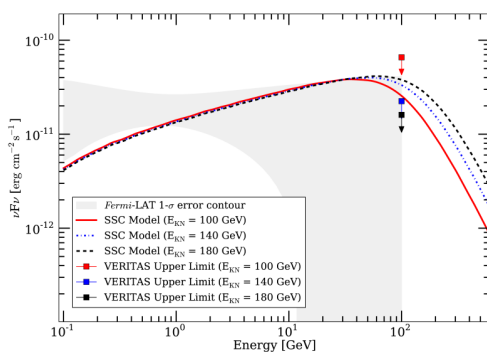


Figure 6. Combined *Fermi*-LAT spectrum including 1σ confidence interval and VERITAS upper limits for the late afterglow of GRB 130427A. Reprinted with permission from Ref. [73].

In parallel to these IACT observations, new EAS facilities, such as ARGO-YBJ, also started taking data in 2004 in the GeV band. No significant VHE emission was reported from any of the events located in the instrument field of view (see, e.g., [74]).

The VHE landscape on GRB study changed dramatically between 2018 and 2019 when the first detections were finally reported by the MAGIC and H.E.S.S. collaborations. These events are described in the following sections and their main parameters are summarized in Table 1.

Table 1. Summary of the main properties of the GRBs detected in the VHE range. GRB 201015A is included due to the strong evidence reported in [75] and is described in Section 4.4. The isotropic energy E_{iso} is calculated in the 50–300 keV range for GRB 180720B, 1–10⁴ keV for GRB 190114C, and 10–10³ keV for GRB 190829A and GRB 201216C. The spectral index α_{obs} is reported for the observed time-integrated spectrum (after absorption due to the EBL) over the whole observation window assuming a power-law model.

Name	T_{90} [s]	Redshift	E_{iso} [erg]	IACT	α_{obs}	E_{max}
180720B	48.9	0.653	6×10^{53}	H.E.S.S.	3.7 ± 1.0	440 GeV
190114C	362	0.4245	3×10^{53}	MAGIC	5.43 ± 0.22	1 TeV
190829A	58.2	0.0785	2×10^{50}	H.E.S.S.	2.59 ± 0.08	3.3 TeV
201216C	48	1.1	5×10^{53}	MAGIC	-	-
201015A	9.8	0.423	10^{50}	MAGIC	-	-

4.1. GRB 190114C

On 14 January 2019, MAGIC detected a very significant (at 50σ level) emission between 300 GeV and 1 TeV from the long GRB 190114C [2]. The event, initially detected by *Swift*-BAT and *Fermi*-GBM, was a bright ($E_{\text{iso}} \sim 3 \times 10^{53}$ erg in the 1–10⁴ keV energy range), a long ($T_{90} = 362$ s as measured by *Swift*-BAT) and quite nearby ($z = 0.4245$) GRB.

Figure 7 shows the timescale of MAGIC follow-up observation: MAGIC received the alert from *Swift*-BAT 22 s after the GRB onset and started observations about 1 min after the GRB trigger under moderate moon conditions and at a relatively high zenith (58°). The GRB was detected with the MAGIC's real-time analysis with a significance of 20σ in the first 20 min of observations above an approximate threshold of 300 GeV. Later, the signal was confirmed up to 50σ -level in the dedicated offline analyses. The detection was reported as quickly as possible to the astrophysical community to strongly encourage the follow-up of this event at other wavelengths. Due to the timescale of early detection, one of the first questions to be answered was if the emission detected by MAGIC was related to the prompt or to the afterglow phase. While the value of T_{90} may indicate that such emission belongs to the prompt, detailed spectral and temporal studies of the keV–MeV data show that at $\sim T_0 + 25$ s the properties of such low-energy emission are more in agreement with the ones of the afterglow phase. This is additionally confirmed by the similar temporal decay index between the X-ray (from *Swift*-XRT between 0.1 and 1 keV) and the VHE (between 300 GeV and 1 TeV) energy light curves (Figure 8). The intrinsic spectrum of the GRB is compatible with a power law with spectral index of $\alpha_{\text{int}} = -2$ between 0.2 and 1 TeV, with no indication of any break or cutoff beyond those energies at the 95% confidence level. Such a flat spectrum shows that the energy output in the VHE range might be considered relevant, turning out to be comparable to the energy release measured at lower energies. Given the high absorption of the VHE flux by the EBL at the redshift of the GRB, the observed spectrum by MAGIC is rather softer and best described by a power law with index $\alpha_{\text{obs}} = -5.43 \pm 0.22$. This was tested against different EBL models, resulting in similar spectral indexes compatible within the statistical uncertainties.

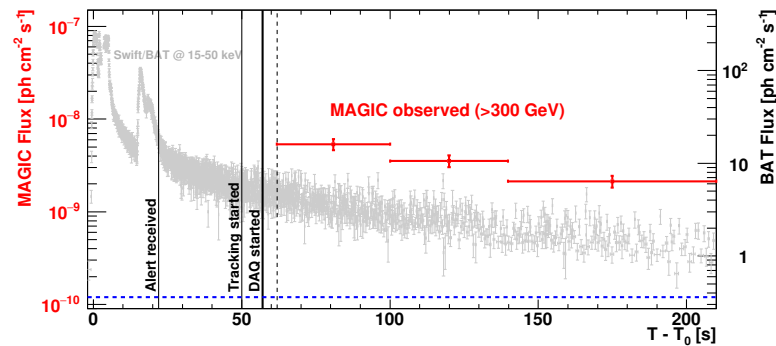


Figure 7. Light curves for MAGIC and *Swift*-BAT. Vertical solid lines show the times of events related to the MAGIC automatic procedure. Extracted from Ref. [2].

The origin of the emission detected by MAGIC is one of the most critical issues. The similarity of the temporal decay in X-ray and VHE energy light curves suggests that the emission processes might be linked and have the same origin. While the simplest hypothesis is that the processes producing the X-ray and VHE photons are the same, namely, synchrotron emission from relativistic electrons accelerated at the external shock in the afterglow of the GRB, this explanation is ruled out if one takes into account that the detected photons largely exceed the synchrotron burn-off limit (see Section 1). Even assuming a Lorentz factor of ~ 1000 , which is not typical for GRBs, the maximum energy of the photons produced by synchrotron is at most around 100 GeV, even considering different density profiles of the interstellar medium density. Therefore, it is reasonable to assume that the VHE emission is due to a different process. In addition, extrapolating the low-energy synchrotron spectrum (from *Fermi*-GBM, *Swift*-XRT, and *Fermi*-LAT data) to VHE range would underestimate the MAGIC flux by approximately one order of magnitude, strengthening the conclusion that the VHE photons are actually produced by a different mechanism. However, the existence of a synchrotron burn-off limit intimately assumes that the radiation came from one single emission region. Having more emission regions might allow synchrotron photons to reach higher energies. In the assumption that the VHE emission is not due to synchrotron, the most simple alternative is the SSC.

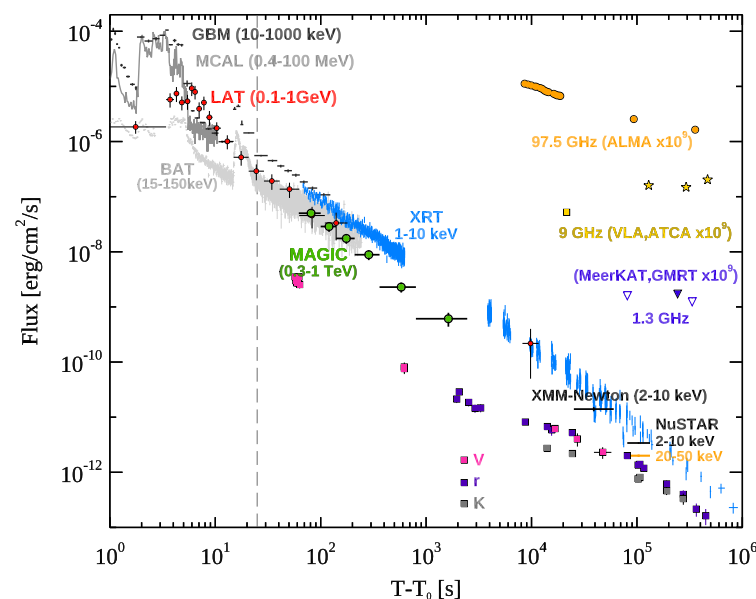


Figure 8. Radio to gamma-ray multi-wavelength light curves of GRB 190114C. The dashed vertical line marks the end of the prompt emission phase. Reprinted with permission from Ref. [76].

The SSC scenario, as commonly observed in other sources such as blazars, foresees a spectral energy distribution (SED) characterized by two distinct emission peaks, one at low energies (X-ray band) due to synchrotron emission, and a second one at higher energies, often in the VHE energy range. The modeling of the GRB 190114C multi-wavelength data with a synchrotron plus SSC emission within the external shock scenario in the afterglow shows exactly these two-peaks features, confirming the presence of an emission component at VHE never observed before (Figure 9). Another remarkable result is the fact that the parameters describing the broadband emission of GRB 190114C have values similar to the ones found in previous studies of GRB afterglows when data only up to the GeV energies were considered. This may hint to the possibility that VHE emission from SSC may be present in all GRBs and that it could be detected by IACTs if favorable conditions apply, i.e., a low enough redshift and good observing conditions. This hypothesis can be confirmed only with the detection of more GRBs in the VHE band.

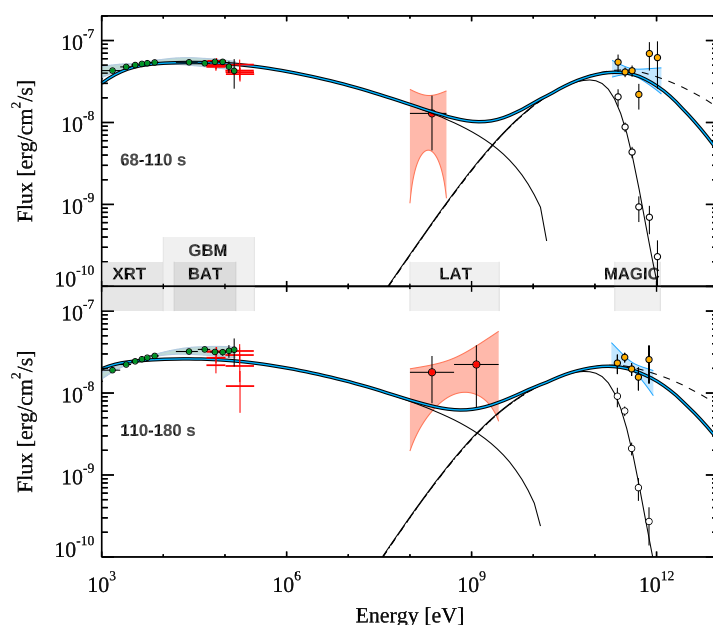


Figure 9. Synchrotron and SSC modeling of the broadband spectra of GRB 190114C in the two time intervals 68–110 s and 110–180 s. Dashed lines represent the SSC emission in the hypothesis of negligible internal $\gamma - \gamma$ opacity. MAGIC points in the VHE band are reported with (empty circles) and without (filled circles) correction for the EBL absorption. From [76].

4.2. GRB 201216C

GRB 201216C was detected by MAGIC [77] after receiving a trigger from *Swift*-BAT [78]. This GRB belongs to the long class as well, and similar to GRB 180720B and GRB 190114C, was very bright, having $E_{\text{iso}} \sim 4.7 \times 10^{53}$ erg in the 10 keV to 1 MeV energy range. GRB 201216C was detected also in optical, where large extinction is present, and its redshift has been estimated to be $z = 1.1$ [79]. MAGIC started the observation of the burst about one minute after the *Swift* trigger, for a total of 2.2 h of exposure. The source was detected with a significance of 5.9σ (post trial) using the first 20 min of data, which makes this the farthest source ever detected. The spectrum in the same time interval can be well described by a power law extending from 50 to 200 GeV, while the energy flux light curve decays monotonically with time [80].

4.3. GRB 180720B and GRB 190829A

GRB 190829A was detected by the *Fermi*-GBM on 29 August 2019 at 19:55:53 UTC [81] with a second detection by *Swift* that occurred 51 s later [82]. The measured redshift of $z = 0.0785$ [83] implies a total isotropic energy release of $\approx 10^{50}$ erg during the prompt phase in both the *Fermi*-GBM and the *Swift* energy bands. This relatively low value placed GRB 190829A on the lower edge of the GRB energy distribution. Nonetheless, the very close-by distance made it a relatively bright GRB in the *Swift*-XRT band. H.E.S.S. observations were performed, starting at $T_0 + 4.3$ h, once afterglow phase emission had already taken over. Follow-up was performed with the use of the four smaller telescopes of the H.E.S.S. array and at a starting zenith angle of $\sim 40^\circ$, corresponding to an energy threshold of ~ 170 GeV. The analysis reported a clear detection of a VHE gamma-ray signal during the first night with statistical significance of 21.7σ in 3.6 h of observation. Surprisingly, the GRB was also detected for the two forthcoming nights at $T_0 + 27.2$ h and $T_0 + 51.2$ h, with statistical significance of 5.5σ and 2.4σ , respectively. Figure 10 (left panel) shows the fading VHE signal measured during the three nights of observations. As for GRB 190114C, the X-ray and VHE gamma-ray light curves also show similar decay profiles with a time evolution characterized by a power law of index $\alpha_{\text{VHE}} = 1.09 \pm 0.05$ and $\alpha_{\text{XRT}} = 1.07 \pm 0.09$ in the H.E.S.S. and *Swift*-XRT bands, respectively. Despite these similarities, the interpretation of the VHE light curve and spectrum of GRB 190829A within the framework of the standard GRB afterglow emission model (such as for GRB 190114C) showed some tensions. The H.E.S.S. data were collected deep in the afterglow phase in a moment in which the bulk Lorentz factor of the outflow was evaluated to be $\Gamma \sim 4.7$ and $\Gamma \sim 2.6$ for the first and second nights of observation, respectively [22,83]. Thus, radiation of few TeV, such as the one measured by H.E.S.S., besides largely exceeding the synchrotron burn-off limit at these specific times, also results in tension with the synchrotron+SSC scenario. With these values of Γ , the electrons producing the VHE emission likely lie in the Klein–Nishina regime. The corresponding reduction in the inverse Compton cross section would introduce a cut-off and a steepening of the flux at VHE. As it appears from H.E.S.S. results (Figure 11), this expected steepening makes it challenging for SSC models to simultaneously reproduce the observed X-ray and VHE spectra [3]. An intriguing possibility is to introduce a leptonic scenario with no limitation placed on the electron maximum energy (and, correspondingly, no synchrotron burn-off limit) that would allow synchrotron emission to produce VHE photons. Although this scenario reproduces the H.E.S.S. data (Figure 11) considerably better, it would require a significant re-evaluation of the relativistic shock-accelerated models. On the other hand, although alternative interpretations have been presented (see, e.g., [84,85]), attempts to model GRB 190829A afterglow using a leptonic synchrotron + SSC emission model have been reported with convincing results and with an obtained set of the shock's microphysical parameters that are similar to those found for GRB 190114C [86].

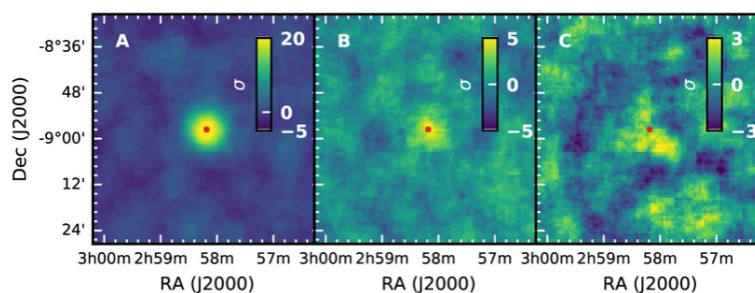


Figure 10. The H.E.S.S. sky map centered at the coordinates of GRB 190829A. The VHE signal was clearly detected for three consecutive nights up to $T_0 + 51$ h. Reprinted with permission from Ref. [3].

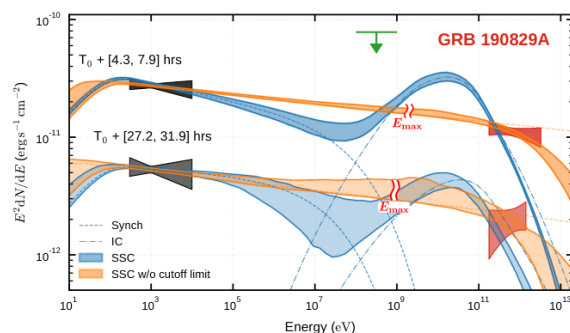


Figure 11. Multi-wavelength models of the first two nights of GRB 190829A H.E.S.S. The black region represents the spectrum and uncertainty of the *Swift*-XRT observations, while the red region is the H.E.S.S. intrinsic spectrum and its uncertainty. The green arrow is the upper limit set by observation during the first night by *Fermi*-LAT. The used model is a standard SSC model with 68% confidence intervals determined from the posterior probability distribution of the model's parameter fitting for the synchrotron component (orange) and the SSC one (blue). No synchrotron cut-off energy (burn-off limit) is considered. Reprinted with permission from Ref. [3].

GRB 180720B was detected by *Fermi*-GBM at 14:21:39.65 UTC [87], and 5 s later by *Swift*-BAT [88]. The event was also detected by the *Fermi*-LAT between T_0 and $T_0 + 700$ s with a maximum photon energy of 5 GeV at $T_0 + 142.4$ s [89]. With a redshift of $z = 0.653$ and an equivalent isotropic energy release of $\sim 6 \times 10^{53}$ erg in the 50–300 keV band, this event is one of the brightest GRBs ever detected by *Fermi*-LAT. The light curves show quite a conventional power-law behavior in both the X and the optical band with a temporal flux decay of index $\alpha_{\text{XRT}} = 1.29 \pm 0.01$ and $\alpha_{\text{optical}} = 1.24 \pm 0.02$. In the HE band, the flux followed a slightly steeper trend with $\alpha_{\text{LAT}} = 0.99 \pm 0.04$, about 1σ from the mean value of the distribution of the decay indices of long GRBs detected by *Fermi*-LAT [1]. Observation by H.E.S.S. started at $T_0 + 10$ h, and the source was detected at $\sim 5\sigma$ level. The detection of a VHE emission at such late times into the afterglow phase implied the presence of very energetic particles accelerated (likely) at the forward shock. Similar to in the case of GRB 190114C, in [1] an SSC-emitting scenario was found to be reasonably in agreement with the observational data, although the marginal level of the significance did not allow more detailed investigation with high statistic and time-resolved spectra and light curve.

4.4. GRB 201015A

GRB 201015A was detected by *Swift*-BAT and followed-up by MAGIC, which reported an excess at the level of $>3\sigma$ in [75,90]. MAGIC observation started from 33 s after T_0 , lasting for about 4 h under good weather conditions. The evidence of emission is found above an energy threshold of ~ 140 GeV. This GRB has some properties similar to GRB 190829A, in particular, the isotropic energy release $E_{\text{iso}} \sim 10^{50}$ erg; however, it is located at a much farther distance $z = 0.423$, resulting in a stronger flux attenuation due to the EBL. With the publication of MAGIC data on this GRB, a more detailed comparison with GRB 190829A will be possible, giving more insights into VHE GRBs with rather low luminosity.

The observations performed by MAGIC and H.E.S.S. established the presence of a VHE emission component in both the early and late afterglow phase. For the former, the fast repositioning and reaction of the MAGIC telescopes played a fundamental role. For the latter, the merit is the well-thought strategy based on observational results from other bands. In both cases, these results have proved to be complementary, providing insights into the nature of GRBs and their VHE detectability at different times, constituting an important lesson for the future observation strategies of next-generation VHE facilities.

5. Advances in GRBs Studies and Open Issues at VHE

The detection of a VHE signal from GRB by MAGIC and H.E.S.S. (particularly GRB 190829A) provided a puzzling and unexpected complexity of scenarios, mainly due to the differences between the phenomenology of the observed events. GRB 190114C and GRB 190829A are events that stand on the opposite edges of the GRB energy distribution being on the $\sim 30\%$ sub-sample of more energetic burst for GRB 190114C ($E_{\text{iso}} = 3 \times 10^{53}$ erg) and more than three orders of magnitude lower for GRB 190829A ($E_{\text{iso}} = 2 \times 10^{50}$ erg). The two events also significantly differ in their temporal profile at VHE, with an extremely bright VHE emission lasting ~ 15 min for GRB 190114C and a dimmer but much longer-lasting emission for GRB 190829A (up to few days after GRB onset). On the other hand, GRB 180720B, which is more similar to GRB 190114C, was detected several hours after the event's onset. In order to exemplify these differences, we reported in Figure 12 (left panel) the value of the bulk Lorentz factor (Γ_0) at the beginning of the afterglow phase, evaluated for a large sample of GRBs [91] once known their isotropic equivalent energy. The positions of the VHE-detected GRBs are overplotted, from which a different nature of GRB 190829A might be pointed out, although both events lie on the so-called Amati relation (Figure 12 right panel). This is an indication that the observed differences in luminosity and energy are not related to a different geometry of the emission (i.e., GRB 190829A is not an off-axis event). On the other hand, gamma rays of such high energies largely exceed the synchrotron burn-off limit, implying the coexistence of an extra emission component in the VHE band. However, the attempt of broadband modeling of the two events led to a different physical interpretation of the VHE emission. While GRB 190114C has been satisfyingly modeled within a synchrotron + SSC emission scenario, the H.E.S.S. collaboration reported an alternative hypothesis for GRB 190829A. In particular, in [3], it was proposed the possibility to interpret the VHE radiation as a synchrotron extending well above the burn-off limit at the time of H.E.S.S. observations. Although intriguing, such an interpretation has been challenged by other works, where, again, a synchrotron+SSC approach seems favorable in modeling the broadband spectrum without requiring peculiar and unconventional choices of the GRB microphysical parameters [86]. Whether an SSC component is at work in all GRBs and which is the maximum energy achievable by different emission mechanisms are still some of the open points that can be addressed with more observations of GRBs at VHE. The tension on the modeling side is also the result of the limited number of VHE GRBs detected up to now, and of the available multi-wavelength (MWL) data collected simultaneously. In particular, *Fermi*-LAT can be of great importance since it covers the energy range where the transition from the synchrotron radiation to the possible SSC component is expected, as exemplified by the case of GRB 190114C. However, such availability of MWL data might not be common, especially if GRBs are detected in the VHE range at late times, when the flux can be below the sensitivity of, e.g., *Fermi*-LAT. Such lack of MWL data can introduce difficulties in the modeling, or lead to degeneracy of the modeling parameters. From this perspective, early VHE follow-up seems to have an advantage, with a higher probability of having more simultaneous MWL data available for later modeling (e.g., the GRB is still bright enough to be detected by instruments such as *Fermi*-LAT). Furthermore, the prompt-to-early-afterglow phase, with the coexistence of forward and reverse shocks in the emitted outflow, could also lead to a large variety of different and interesting emitting scenarios in the VHE band. In this regard, while a deeper understanding of the afterglow phase at VHE is due, one of the next challenges is the detection of VHE emission in the prompt phase. The debate on the physical process at the origin of the prompt emission is still open, with different possibilities missing a clear observational proof. A detection of the prompt emission in the VHE range could resolve such a long-lasting issue, giving a new perspective on this poorly known phase of GRBs. The challenge for IACTs is the short duration of the prompt phase, compared to the delivery times of the alerts from triggering instruments and the time for their reaction. In particular, T_{90} alone is not a good indicator of the duration of the prompt phase and of the nature of a GRB, as already debated within the GRB community (see, e.g., [92,93]). Therefore,

long-duration GRBs with T_{90} of the order of hundreds of seconds (e.g., GRB 190114C) can also have prompt phases with a much shorter duration, as shown by the spectral and temporal analysis of the GRB light curves. For this reason, ground-based instruments such as HAWC (<https://www.hawc-observatory.org/>) (that already reported results on GRB observations [94]), LHAASO (<http://english.ihep.cas.cn/lhaaso/>), and the future SWGO (<https://www.swgo.org/SWGOWiki/doku.php>) (all websites accessed on 10 April 2022) could be more suited, given their high-duty cycle and sky coverage, with the downside of a higher energy threshold.

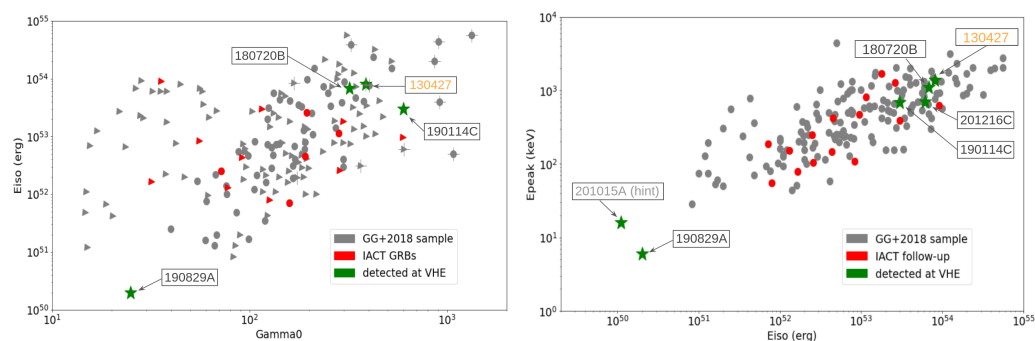


Figure 12. Left panel: Correlation between the bulk Lorentz factor at the beginning of the afterglow phase (Γ_0) and the isotropic equivalent energy E_{iso} for the sample of GRB reported in [91]. Right panel: the empirical correlation (Amati relation) between the isotropic equivalent energy E_{iso} and the peak energy of the GRB spectrum for the same sample in [91] and for the events detected in the VHE band. In both panels, GRBs followed-up by IACTs are denoted by green and red symbols, indicating those with and without detection, respectively. Reprinted with permission from Ref. [95].

An additional challenge for IACTs is the detection of short GRBs. While they are located (on average) at smaller redshift with respect to long GRBs, they are also less luminous, making a detection with IACTs difficult. Currently, the strongest evidence for a VHE emission component from short GRBs was reported by MAGIC for GRB 160821B [96]. The telescope's fast response played a major role, despite the adverse observational conditions (reduced atmospheric conditions, relatively high zenith of the observation, and increased night sky background due to the presence of the Moon). A signal at the level of 3σ (post-trial) was found with a flux upper limit of $1.1 \times 10^{-11} \text{ cm}^{-2} \text{ s}^{-1}$ in the first half hour, giving the possibility to perform interesting studies on the expected energy flux at VHE in an MWL context [96]. The SSC model was found to be in tension with the data, nonetheless a firm detection and a higher statistics is needed to rule out this possibility. Such a discovery would be of utmost importance to understand if there are similarities at VHE between long and short GRBs. Moreover, short GRBs are intimately connected with searches of gravitational waves (GWs) from their progenitors. A coincident detection of a short GRB and GWs would allow a comprehensive picture of the system leading to the GRB itself, and of its following evolution.

Finally, the detection of other GRBs at VHE can open up the possibility of interesting studies on more fundamental topics. VHE signal from these events might be extremely valuable for probing external $\gamma - \gamma$ absorption due to the EBL out to larger redshifts than the ones that can be typically reached with other extragalactic sources, such as blazars. Another possibility could involve the searches for Lorentz invariance violation (LIV), where distant GRBs with high-energy photons can considerably improve the sensitivity of the resulting lower limit (see, e.g., [97] for a LIV study using GRB 190114C data). VHE GRB data can also be used for the search of axion-like particles (ALPs), where we expect spectral signatures and a reduction of the optical depth, leading to a lower absorption with respect to the expectation from the EBL (see, e.g., [98]). The GRBs detected so far at VHE confirmed that a low–moderate redshift is still a necessary condition for the detection for current IACTs, especially if the luminosity is towards the low end of the distribution. GRB 201216C,

detected at $z = 1.1$, stands as an outsider and can represent an interesting case study for possible EBL or LIV studies. This is indeed a promising result for the next generation of Cherenkov telescopes that, thanks to improved sensitivity and energy threshold, might further extend the gamma-ray horizon of these observations.

6. The Next Decades

The Cherenkov Telescope Array Observatory (CTAO) represents the next-generation ground-based observatory for the study of VHE gamma rays. It will consist of two arrays, one for each hemisphere, made up of IACTs of different size and characteristics. The CTA array will routinely perform follow-up observations of GRB triggers and other transients objects also coming from other cosmic signal, such as neutrino and gravitational waves [99]. The estimation of the detection prospects for such observations are necessarily still preliminary and are dependent on the final array layout and performance. Nonetheless, even starting with simplified assumptions about the GRB emission, the CTA Consortium already reported the possibility of detecting \sim hundreds (or more) of photons from moderate to bright GRB, allowing for a significant improvement in the photon statistics and for the possibility to have good-quality time-resolved spectra [100]. The preliminary results reported in such a study show the possibility of detecting up to few GRB per year (considering both arrays) and allowing to move rapidly from the single-case GRB study, such as for current IACT, to a full GRB population study at VHE. In order to confirm these early results and achieve a step forward in the determination of CTA's prospects for GRB follow-ups, the CTA Consortium is currently working on a new study where the potential detection rate is estimated using a theoretical-based approach. Such an approach is based on the *POpulation Synthesis Theory Integrated code for Very high energy Emission* (POSyTIVE) model for GRBs [101]. The aim is to build a GRB population based on few intrinsic properties and assumptions such as E_{peak} and redshift distribution, $E_{\text{peak}}-E_{\text{iso}}$ correlation (Amati relation) [102], and the bulk Lorentz factor distribution obtained by measured the time of the afterglow onset (providing the bulk Lorentz factor of the event's coasting phase). The population obtained (for both long and short GRBs) is calibrated against a wide dataset of multi-wavelength observations. In order to derive the final expected spectrum, both the prompt and the afterglow emission are simulated according to a standard leptonic synchrotron+SSC emission model [14]. The GRB spectra obtained are then used to simulate the detailed CTA response through the use of dedicated analysis pipelines based on *gammapy* (<https://gammapy.org/>) and *ctools* (<http://cta.irap.omp.eu/ctools/>) (accessed on 27 April 2022) and making use of the most recent instrument response functions (IRFs). The results of this study are expected by the end of 2022.

In the framework of the CTA, the earliest science operations have recently started thanks to the large-sized telescope prototype (LST-1). LSTs are the largest telescopes designed for CTA, having a 23 m diameter reflector. The first prototype, LST-1 (Figure 13 left panel), is located at the Roque de los Muchachos observatory (28.8° N, 17.8° W, 2200 m a.s.l.), on the Canary Island of La Palma [103], the designed site for the CTA north array. Thanks to the reflective surface of about 400 m^2 , the LST-1 will be able to achieve an energy threshold of $\approx 20 \text{ GeV}$, a value particularly suitable for transients and high-redshift source observations. Furthermore, LSTs are built with a light carbon-fiber structure in order to reduce the total weight of the telescope to about 103 tons and to make possible the fast repositioning ($\sim 30 \text{ s}$ for 180° azimuth displacement) to catch early emission phases of transient objects. LST-1 was inaugurated in October 2018 and is currently finalizing its commissioning phase. Starting from the first months of 2021, the time allocated for technical observations has been gradually reduced, allowing the first observations of targets of astrophysical interest. Transients follow-up, including GRBs, have the highest priority among LST-1 observed targets. Although a fully automatic procedure that will allow the telescope to react automatically to incoming alerts is still under development, the first observations of GRBs have been performed [95]. Preliminary analysis did not reveal VHE emission associated with any of the observed alerts; however, the continuous effort in

improving the telescope's performance and robustness will soon place LST-1 in a key position for VHE observations of those peculiar events, making it a noticeable testbench for the forthcoming full-configured CTA array.

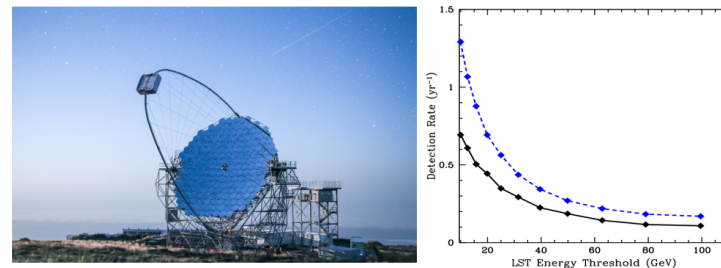


Figure 13. (Left) The LST prototype during night operation in La Palma. Picture credit: Tomohiro Inada. (Right) GRB detection rate for one of the CTA arrays as a function of the expected LST energy threshold. The curves represent two possible empirical assumptions for GRB spectrum at very high energy; one considering a simple extrapolation of the band emission up to VHE (solid black), the other considering an additional emission component (dashed blue). Reprinted with permission from Ref. [100].

The firm detection of a signal extending up to the multi-TeV band for GRB 190829A has opened new interesting possibilities for observations also with IACTs not specifically designed for transients follow-up, such as the small-sized telescopes (SST) foreseen for the CTA. An interesting example is the case of the ASTRI mini-array, composed of nine imaging atmospheric dual-mirror Cherenkov telescopes at the Teide Observatory site on the Canary Island of La Palma [104]. The telescopes will have a relatively small primary mirror of ~ 4 m diameter, allowing to detect gamma rays in the 0.5–200 TeV range. Despite the corresponding limited gamma-ray horizon accessible, the authors in [105] proved the feasibility of the ASTRI mini-array to detect bright and nearby GRBs. This would guarantee to cover, with high sensitivity, the extreme edge of the VHE band, complementing the data collected at lower energies with instruments such as the LSTs.

7. Conclusions

VHE observations provide a new channel to study the physics of GRBs in an energy range particularly important for the discrimination of different emitting scenarios and for the constraint of the GRBs' physical parameters in space. The detection of GRBs at VHE represents one of the major breakthroughs for transient astrophysics in the last years. This result was finally achieved thanks to the relentless efforts and the continuous improvements on both the technical and the observational strategy side by current IACTs collaborations. The small sample of detected events shows a large variety of phenomenology that leaves some questions unanswered, creating difficulties in finding a possible common interpretative scenarios. In all detected events, VHE emission has been observed on timescales much longer than the corresponding prompt phase, confirming the results already observed in the GeV band. However, besides the detection of bright and powerful events, that for a long time were assumed to be the best candidates for VHE emission, relatively low-luminosity events also showed long-lasting emission up to the TeV band. This suggests that the detection of these GRBs is likely not unique and the VHE component might be a relatively common feature of many GRBs, although observable only under favorable conditions by IACTs. Whether *all* GRBs have a VHE emission component and whether the parameter space of a possible VHE-emitter GRB is larger than what was previously thought, this will be one of the key issues for the next generation of IACTs, namely, the CTAO. Short timescale transients (including GRBs) have been one of the key motivations when designing the different elements of the CTA, and in particular the LSTs, whose first prototype recently started its operation in the Canary Island of La Palma. Once fully configured, a detection rate of the order of a few bursts per year might be expected, allowing us to build and

characterize the GRB population at VHE. Furthermore, the achievable photon statistics would allow CTA to study the spectral and temporal properties of GRBs, shedding light into unresolved issues such as determining the jet formation dynamics and the mechanisms of particle acceleration.

Author Contributions: The authors contributed equally to this work. The authors have read and agreed to the published version of the manuscript.

Funding: This research received no external funding.

Institutional Review Board Statement: Not applicable.

Informed Consent Statement: Not applicable.

Data Availability Statement: Not applicable.

Acknowledgments: The authors acknowledge the anonymous referees for their useful comments.

Conflicts of Interest: The authors declare no conflict of interest.

References

1. Abdalla, H.; Adam, R.; Aharonian, F.; Ait Benkhali, F.; Angüner, E.O.; Arakawa, M.; Arcaro, C.; Armand, C.; Ashkar, H.; Backes, M.; et al. A very-high-energy component deep in the γ -ray burst afterglow. *Nature* **2019**, *575*, 464–467. [[CrossRef](#)]
2. MAGIC Collaboration. Teraelectronvolt emission from the γ -ray burst GRB 190114C. *Nature* **2019**, *575*, 455–458. [[CrossRef](#)]
3. H.E.S.S. Collaboration; Abdalla, H.; Aharonian, F.; Ait Benkhali, F.; Angüner, E.O.; Arcaro, C.; Armand, C.; Armstrong, T.; Ashkar, H.; Backes, M.; et al. Revealing X-ray and gamma ray temporal and spectral similarities in the GRB 190829A afterglow. *Science* **2021**, *372*, 1081–1085. [[CrossRef](#)]
4. Carosi, A.; Antonelli, A.; Becerra Gonzalez, J.; Berti, A.; Covino, S.; Garczarczyk, M.; Gaug, M.; Lombardi, S.; Longo, F.; Moretti, E.; et al. Recent follow-up observations of GRBs in the very high energy band with the MAGIC Telescopes. In Proceedings of the 34th International Cosmic Ray Conference (ICRC2015), The Hague, The Netherlands, 30 July–6 August 2015; International Cosmic Ray Conference; Volume 34, p. 809.
5. Aleksić, J.; Ansoldi, S.; Antonelli, L.A.; Antoranz, P.; Babic, A.; Barres de Almeida, U.; Barrio, J.A.; Becerra González, J.; Bednarek, W.; Berger, K.; et al. MAGIC upper limits on the GRB 090102 afterglow. *Mon. Not. R. Astron. Soc.* **2014**, *437*, 3103–3111. [[CrossRef](#)]
6. Paczynski, B. Gamma-ray bursters at cosmological distances. *Astrophys. J. Lett.* **1986**, *308*, L43–L46. [[CrossRef](#)]
7. Thompson, C. A model of gamma-ray bursts. *Mon. Not. R. Astron. Soc.* **1994**, *270*, 480–498. [[CrossRef](#)]
8. Granot, J. Gamma-Ray Bursts from Magnetic Reconnection: Variability and Robustness of Light Curves. *Astrophys. J. Lett.* **2016**, *816*, L20. [[CrossRef](#)]
9. Band, D.; Matteson, J.; Ford, L.; Schaefer, B.; Palmer, D.; Teegarden, B.; Cline, T.; Briggs, M.; Paciesas, W.; Pendleton, G.; et al. BATSE Observations of Gamma-Ray Burst Spectra. I. Spectral Diversity. *Astrophys. J.* **1993**, *413*, 281. [[CrossRef](#)]
10. Toffano, M.; Ghirlanda, G.; Nava, L.; Ghisellini, G.; Ravaio, M.E.; Oganessian, G. The slope of the low-energy spectrum of prompt gamma-ray burst emission. *Astropart. Astrophys.* **2021**, *652*, A123. [[CrossRef](#)]
11. Basak, R.; Rao, A.R. Discovery of Smoothly Evolving Blackbodies in the Early Afterglow of GRB 090618: Evidence for a Spine-Sheath Jet? *Astrophys. J.* **2015**, *812*, 156. [[CrossRef](#)]
12. Cohen, E.; Katz, J.I.; Piran, T.; Sari, R.; Preece, R.D.; Band, D.L. Possible Evidence for Relativistic Shocks in Gamma-Ray Bursts. *Astrophys. J.* **1997**, *488*, 330–337. [[CrossRef](#)]
13. Ghirlanda, G.; Celotti, A.; Ghisellini, G. Extremely hard GRB spectra prune down the forest of emission models. *Astropart. Astrophys.* **2003**, *406*, 879–892. [[CrossRef](#)]
14. Sari, R.; Esin, A.A. On the Synchrotron Self-Compton Emission from Relativistic Shocks and Its Implications for Gamma-Ray Burst Afterglows. *Astrophys. J.* **2001**, *548*, 787–799. [[CrossRef](#)]
15. Zhang, B.; Mészáros, P. High-Energy Spectral Components in Gamma-Ray Burst Afterglows. *Astrophys. J.* **2001**, *559*, 110–122. [[CrossRef](#)]
16. Gupta, N.; Zhang, B. Prompt emission of high-energy photons from gamma ray bursts. *Mon. Not. R. Astron. Soc.* **2007**, *380*, 78–92. [[CrossRef](#)]
17. Atwood, W.B.; Abdo, A.A.; Ackermann, M.; Althouse, W.; Anderson, B.; Axelsson, M.; Baldini, L.; Ballet, J.; Band, D.L.; Barbiellini, G.; et al. The Large Area Telescope on the Fermi Gamma-Ray Space Telescope Mission. *Astrophys. J.* **2009**, *697*, 1071–1102. [[CrossRef](#)]
18. Ghisellini, G.; Ghirlanda, G.; Nava, L.; Celotti, A. GeV emission from gamma-ray bursts: a radiative fireball? *Mon. Not. R. Astron. Soc.* **2010**, *403*, 926–937. [[CrossRef](#)]
19. Piran, T. Gamma-ray bursts and the fireball model. *Phys. Rep.* **1999**, *314*, 575–667. [[CrossRef](#)]

20. Abdo, A.A.; Ackermann, M.; Arimoto, M.; Asano, K.; Atwood, W.B.; Axelsson, M.; Baldini, L.; Ballet, J.; Band, D.L.; Barbiellini, G.; et al. Fermi Observations of High-Energy Gamma-Ray Emission from GRB 080916C. *Science* **2009**, *323*, 1688. [[CrossRef](#)]
21. Ackermann, M.; Asano, K.; Atwood, W.B.; Axelsson, M.; Baldini, L.; Ballet, J.; Barbiellini, G.; Baring, M.G.; Bastieri, D.; Bechtol, K.; et al. Fermi Observations of GRB 090510: A Short-Hard Gamma-ray Burst with an Additional, Hard Power-law Component from 10 keV TO GeV Energies. *Astrophys. J.* **2010**, *716*, 1178–1190. [[CrossRef](#)]
22. Blandford, R.D.; McKee, C.F. Fluid dynamics of relativistic blast waves. *Phys. Fluids* **1976**, *19*, 1130–1138. [[CrossRef](#)]
23. Guetta, D.; Granot, J. High-Energy Emission from the Prompt Gamma-Ray Burst. *Astrophys. J.* **2003**, *585*, 885–889. [[CrossRef](#)]
24. Guetta, D.; Granot, J. Observational implications of a plerionic environment for gamma-ray bursts. *Mon. Not. R. Astron. Soc.* **2003**, *340*, 115–138. [[CrossRef](#)]
25. Daigne, F.; Bošnjak, Ž.; Dubus, G. Reconciling observed gamma-ray burst prompt spectra with synchrotron radiation? *Astron. Astrophys.* **2011**, *526*, A110, [[CrossRef](#)]
26. Bošnjak, Ž.; Daigne, F.; Dubus, G. Prompt high-energy emission from gamma-ray bursts in the internal shock model. *Astron. Astrophys.* **2009**, *498*, 677–703. [[CrossRef](#)]
27. Daigne, F. *High-Energy Emission from Gamma-Ray Bursts*; International Journal of Modern Physics Conference Series; World Scientific: Singapore, 2012; Volume 8, pp. 196–208. [[CrossRef](#)]
28. Razaque, S. Modeling and Interpretation of High Energy Emission from GRBs Observed with the Fermi Gamma Ray Space Telescope. In Proceedings of the APS April Meeting Abstracts, Denver, Colorado, 2–5 May 2009; p. W8.003.
29. Asano, K.; Inoue, S.; Mészáros, P. Prompt High-Energy Emission from Proton-Dominated Gamma-Ray Bursts. *Astrophys. J.* **2009**, *699*, 953–957. [[CrossRef](#)]
30. Beniamini, P.; Nava, L.; Duran, R.B.; Piran, T. Energies of GRB blast waves and prompt efficiencies as implied by modelling of X-ray and GeV afterglows. *Mon. Not. R. Astron. Soc.* **2015**, *454*, 1073–1085. [[CrossRef](#)]
31. Wang, X.Y.; He, H.N.; Li, Z.; Wu, X.F.; Dai, Z.G. Klein-Nishina Effects on the High-energy Afterglow Emission of Gamma-ray Bursts. *Astrophys. J.* **2010**, *712*, 1232–1240. [[CrossRef](#)]
32. Liu, R.Y.; Wang, X.Y.; Wu, X.F. Interpretation of the Unprecedentedly Long-lived High-energy Emission of GRB 130427A. *Astrophys. J. Lett.* **2013**, *773*, L20, [[CrossRef](#)]
33. Wang, X.Y.; Dai, Z.G.; Lu, T. Prompt High-Energy Gamma-Ray Emission from the Synchrotron Self-Compton Process in the Reverse Shocks of Gamma-Ray Bursts. *Astrophys. J. Lett.* **2001**, *546*, L33–L37, [[CrossRef](#)]
34. Granot, J.; Guetta, D. Explaining the High-Energy Spectral Component in GRB 941017. *Astrophys. J. Lett.* **2003**, *598*, L11–L14, [[CrossRef](#)]
35. Böttcher, M.; Dermer, C.D. High-energy Gamma Rays from Ultra-high-energy Cosmic-Ray Protons in Gamma-Ray Bursts. *Astrophys. J. Lett.* **1998**, *499*, L131–L134, [[CrossRef](#)]
36. Nava, L. High-energy emission from gamma-ray bursts. *Int. J. Mod. Phys. D* **2018**, *27*, 1842003, [[CrossRef](#)]
37. Hurley, K.; Dingus, B.L.; Mukherjee, R.; Sreekumar, P.; Kouveliotou, C.; Meegan, C.; Fishman, G.J.; Band, D.; Ford, L.; Bertsch, D.; et al. Detection of a γ -ray burst of very long duration and very high energy. *Nature* **1994**, *372*, 652–654. [[CrossRef](#)]
38. Merck, M.; Bertsch, D.L.; Dingus, B.L.; Fichtel, C.E.; Hartman, R.C.; Hunter, S.D.; Kanbach, G.; Kniffen, D.A.; Lin, Y.C.; Mayer-Hasselzander, H.A.; et al., Observations of High-Energy Gamma-ray Bursts with EGRET. In *IAU Colloq. 151: Flares and Flashes*; Springer: Berlin/Heidelberg, Germany 1995; Volume 454, p. 358. [[CrossRef](#)]
39. González, M.M.; Dingus, B.L.; Kaneko, Y.; Preece, R.D.; Dermer, C.D.; Briggs, M.S. A γ -ray burst with a high-energy spectral component inconsistent with the synchrotron shock model. *Nature* **2003**, *424*, 749–751. [[CrossRef](#)]
40. Tavani, M.; Barbiellini, G.; Argan, A.; Boffelli, F.; Bulgarelli, A.; Caraveo, P.; Cattaneo, P.W.; Chen, A.W.; Cocco, V.; Costa, E.; et al. The AGILE Mission. *Astron. Astrophys.* **2009**, *502*, 995–1013. [[CrossRef](#)]
41. Giuliani, A.; Mereghetti, S.; Fornari, F.; Del Monte, E.; Feroci, M.; Marisaldi, M.; Esposito, P.; Perotti, F.; Tavani, M.; Argan, A.; et al. AGILE detection of delayed gamma-ray emission from GRB 080514B. *Astron. Astrophys.* **2008**, *491*, L25–L28, [[CrossRef](#)]
42. Del Monte, E.; Barbiellini, G.; Donnarumma, I.; Fuschino, F.; Giuliani, A.; Longo, F.; Marisaldi, M.; Pucella, G.; Tavani, M.; Trifoglio, M.; et al. The AGILE observations of the hard and bright GRB 100724B. *Astron. Astrophys.* **2011**, *535*, A120, [[CrossRef](#)]
43. Longo, F.; Moretti, E.; Nava, L.; Desiante, R.; Olivo, M.; Del Monte, E.; Rappoldi, A.; Fuschino, F.; Marisaldi, M.; Giuliani, A.; et al. Upper limits on the high-energy emission from gamma-ray bursts observed by AGILE-GRID. *Astron. Astrophys.* **2012**, *547*, A95. [[CrossRef](#)]
44. Meegan, C.; Lichti, G.; Bhat, P.N.; Bissaldi, E.; Briggs, M.S.; Connaughton, V.; Diehl, R.; Fishman, G.; Greiner, J.; Hoover, A.S.; et al. The Fermi Gamma-ray Burst Monitor. *Astrophys. J.* **2009**, *702*, 791–804. [[CrossRef](#)]
45. Abdo, A.A.; Ackermann, M.; Asano, K.; Atwood, W.B.; Axelsson, M.; Baldini, L.; Ballet, J.; Band, D.L.; Barbiellini, G.; Bastieri, D.; et al. Fermi Observations of High-energy Gamma-ray Emission from GRB 080825C. *Astrophys. J.* **2009**, *707*, 580–592. [[CrossRef](#)]
46. Abdo, A.A.; Ackermann, M.; Ajello, M.; Asano, K.; Atwood, W.B.; Axelsson, M.; Baldini, L.; Ballet, J.; Barbiellini, G.; Bastieri, D.; et al. Fermi Detection of Delayed GeV Emission from the Short Gamma-Ray Burst 081024B. *Astrophys. J.* **2010**, *712*, 558–564. [[CrossRef](#)]
47. Giuliani, A.; Fuschino, F.; Vianello, G.; Marisaldi, M.; Mereghetti, S.; Tavani, M.; Cutini, S.; Barbiellini, G.; Longo, F.; Moretti, E.; et al. AGILE Detection of Delayed Gamma-ray Emission From the Short Gamma-Ray Burst GRB 090510. *Astrophys. J.* **2010**, *708*, L84–L88, [[CrossRef](#)]

48. Fan, Y.Z.; Piran, T.; Narayan, R.; Wei, D.M. High-energy afterglow emission from gamma-ray bursts. *Mon. Not. R. Astron. Soc.* **2008**, *384*, 1483–1501. [[CrossRef](#)]
49. Asano, K.; Guiriec, S.; Mészáros, P. Hadronic Models for the Extra Spectral Component in the Short GRB 090510. *Astrophys. J. Lett.* **2009**, *705*, L191–L194. [[CrossRef](#)]
50. Ackermann, M.; Ajello, M.; Asano, K.; Atwood, W.B.; Axelsson, M.; Baldini, L.; Ballet, J.; Barbiellini, G.; Baring, M.G.; Bastieri, D.; et al. Fermi-LAT Observations of the Gamma-Ray Burst GRB 130427A. *Science* **2014**, *343*, 42–47. [[CrossRef](#)]
51. Kouveliotou, C.; Granot, J.; Racusin, J.L.; Bellm, E.; Vianello, G.; Oates, S.; Fryer, C.L.; Boggs, S.E.; Christensen, F.E.; Craig, W.W.; et al. NuSTAR Observations of GRB 130427A Establish a Single Component Synchrotron Afterglow Origin for the Late Optical to Multi-GeV Emission. *Astrophys. J. Lett.* **2013**, *779*, L1. [[CrossRef](#)]
52. Ackermann, M.; Ajello, M.; Asano, K.; Axelsson, M.; Baldini, L.; Ballet, J.; Barbiellini, G.; Bastieri, D.; Bechtol, K.; Bellazzini, R.; et al. The First Fermi-LAT Gamma-Ray Burst Catalog. *Astrophys. J. Suppl.* **2013**, *209*, 11. [[CrossRef](#)]
53. Weekes, T.C.; Cawley, M.F.; Fegan, D.J.; Gibbs, K.G.; Hillas, A.M.; Kowk, P.W.; Lamb, R.C.; Lewis, D.A.; Macomb, D.; Porter, N.A.; et al. Observation of TeV Gamma Rays from the Crab Nebula Using the Atmospheric Cerenkov Imaging Technique. *Astrophys. J.* **1989**, *342*, 379. [[CrossRef](#)]
54. Boella, G.; Butler, R.C.; Perola, G.C.; Piro, L.; Scarsi, L.; Bleeker, J.A.M. BeppoSAX, the wide band mission for X-ray astronomy. *Astron. Astrophys. Suppl.* **1997**, *122*, 299–307. [[CrossRef](#)]
55. Hurley, K.; Sommer, M.; Boer, M.; Niel, M.; Laros, J.; Fenimore, E.; Klebesadel, R.; Fishman, G.; Kouveliotou, C.; Meegan, C.; et al. ULYSSES precise localizations of gamma-ray bursts. *Astropart. Astrophys.* **1993**, *97*, 39–41.
56. Alexandreas, D.E.; Allen, G.E.; Berley, D.; Biller, S.; Burman, R.L.; Cavalli-Sforza, M.; Chang, C.Y.; Chen, M.L.; Chumney, P.; Coyne, D.; et al. *Search for Ultra High Energy Radiation from Gamma-Ray Bursts*; Gamma-Ray Bursts; Fishman, G.J., Ed.; American Institute of Physics Conference Series; American Institute of Physics: College Park, MD, USA, 1994; Volume 307, pp. 481–485.
57. Padilla, L.; Funk, B.; Krawczynski, H.; Contreras, J.L.; Moralejo, A.; Aharonian, F.; Akhperjanian, A.G.; Barrio, J.A.; Beteta, J.G.; Cortina, J.; et al. Search for gamma-ray bursts above 20 TeV with the HEGRA AIROBICC Cherenkov array. *Astron. Astrophys.* **1998**, *337*, 43–50.
58. Catanese, M.; Chantell, M.; Covault, C.E.; Cronin, J.W.; Fick, B.E.; Fortson, L.F.; Fowler, J.W.; Gibbs, K.G.; Glasmacher, M.A.K.; Green, K.D.; et al. Search for Ultra High Energy (UHE) γ -ray counterparts of BATSE 3B catalog events. In *Gamma-ray Bursts: 3rd Huntsville Symposium*; Kouveliotou, C., Briggs, M.F., Fishman, G.J., Eds.; American Institute of Physics Conference Series; American Institute of Physics: College Park, MD, USA, 1996; Volume 384, pp. 598–602. [[CrossRef](#)]
59. Aglietta, M.; Alessandro, B.; Antonioli, P.; Arneodo, F.; Bergamasco, L.; Bertaina, M.; Castagnoli, C.; Castellina, A.; Chiavassa, A.; Cini, G.; et al. Search for high energy GRBs with EASTOP. *Astron. Astrophys.* **1999**, *138*, 595–596. [[CrossRef](#)]
60. Atkins, R.; Benbow, W.; Berley, D.; Chen, M.L.; Coyne, D.G.; Delay, R.S.; Dingus, B.L.; Dorfan, D.E.; Ellsworth, R.W.; Espinoza, C.; et al. Milagrito, a TeV air-shower array. *Nucl. Instrum. Methods Phys. Res. A* **2000**, *449*, 478–499. [[CrossRef](#)]
61. Atkins, R.; Benbow, W.; Berley, D.; Chen, M.L.; Coyne, D.G.; Dingus, B.L.; Dorfan, D.E.; Ellsworth, R.W.; Evans, D.; Falcone, A.; et al. The High-Energy Gamma-Ray Fluence and Energy Spectrum of GRB 970417a from Observations with Milagrito. *Astrophys. J.* **2003**, *583*, 824–832. [[CrossRef](#)]
62. Connaughton, V.; Ackerlof, C.W.; Barthelmy, S.; Biller, S.; Boyle, P.; Buckley, J.; Carter-Lewis, D.A.; Cantanese, M.; Cawley, M.F.; Cline, T.; et al. A Search for TeV Counterparts to BATSE Gamma-Ray Bursts. *Astrophys. J.* **1997**, *479*, 859–867. [[CrossRef](#)]
63. Gehrels, N.; Chincarini, G.; Giommi, P.; Mason, K.O.; Nousek, J.A.; Wells, A.A.; White, N.E.; Barthelmy, S.D.; Burrows, D.N.; Cominsky, L.R.; et al. The Swift Gamma-Ray Burst Mission. *Astrophys. J.* **2004**, *611*, 1005–1020. [[CrossRef](#)]
64. Gehrels, N.; Razzaque, S. Gamma-ray bursts in the swift-Fermi era. *Front. Phys.* **2013**, *8*, 661–678. [[CrossRef](#)]
65. Albert, J.; Aliu, E.; Anderhub, H.; Antoranz, P.; Armada, A.; Baixeras, C.; Barrio, J.A.; Bartko, H.; Bastieri, D.; Becker, J.; et al. MAGIC Upper Limits on the Very High Energy Emission from Gamma-Ray Bursts. *Astrophys. J.* **2007**, *667*, 358–366. [[CrossRef](#)]
66. Albert, J.; Aliu, E.; Anderhub, H.; Antoranz, P.; Armada, A.; Asensio, M.; Baixeras, C.; Barrio, J.A.; Bartelt, M.; Bartko, H.; et al. Flux Upper Limit on Gamma-Ray Emission by GRB 050713a from MAGIC Telescope Observations. *Astrophys. J. Lett.* **2006**, *641*, L9–L12. [[CrossRef](#)]
67. Berti, A.; Antonelli, L.A.; Bosnjak, Z.; Cortina, J.; Covino, S.; D’Elia, V.; Espiñeira, E.d.S.; Fukami, S.; Inoue, S.; Longo, F.; et al. Searching for GRBs at VHE with MAGIC: the status before CTA. In *Proceedings of the 36th International Cosmic Ray Conference (ICRC2019)*, Madison, WI, USA, 25 July–1 August 2019; International Cosmic Ray Conference; Volume 36, p. 634.
68. Aleksić, J.; Anderhub, H.; Antonelli, L.A.; Antoranz, P.; Backes, M.; Baixeras, C.; Balestra, S.; Barrio, J.A.; Bastieri, D.; Becerra González, J.; et al. MAGIC observation of the GRB 080430 afterglow. *Astron. Astrophys.* **2010**, *517*, A5. [[CrossRef](#)]
69. Aharonian, F.; Akhperjanian, A.G.; Barres de Almeida, U.; Bazer-Bachi, A.R.; Behera, B.; Benbow, W.; Bernlöhr, K.; Boisson, C.; Bochow, A.; Borrel, V.; et al. HESS observations of γ -ray bursts in 2003–2007. *Astron. Astrophys.* **2009**, *495*, 505–512. [[CrossRef](#)]
70. Aharonian, F.; Akhperjanian, A.G.; Barres DeAlmeida, U.; Bazer-Bachi, A.R.; Behera, B.; Beilicke, M.; Benbow, W.; Bernlöhr, K.; Boisson, C.; Borrel, V.; et al. HESS Observations of the Prompt and Afterglow Phases of GRB 060602B. *Astrophys. J.* **2009**, *690*, 1068–1073. [[CrossRef](#)]
71. H.E.S.S. Collaboration; Abramowski, A.; Aharonian, F.; Ait Benkhali, F.; Akhperjanian, A.G.; Angüner, E.; Anton, G.; Balenderan, S.; Balzer, A.; Barnacka, A.; et al. Search for TeV Gamma-ray Emission from GRB 100621A, an extremely bright GRB in X-rays, with H.E.S.S. *Astron. Astrophys.* **2014**, *565*, A16. [[CrossRef](#)]

72. Hoischen, C.; Balzer, A.; Bissaldi, E.; Füßling, M.; Garrigoux, T.; Gottschall, D.; Holler, M.; Mitchell, A.; O'Brien, P.; Parsons, R.; et al. GRB Observations with H.E.S.S. II. In Proceedings of the 35th International Cosmic Ray Conference (ICRC2017), Busan, Korea, 12–20 July 2017; International Cosmic Ray Conference; Volume 301, p. 636.
73. Aliu, E.; Aune, T.; Barnacka, A.; Beilicke, M.; Benbow, W.; Berger, K.; Biteau, J.; Buckley, J.H.; Bugaev, V.; Byrum, K.; et al. Constraints on Very High Energy Emission from GRB 130427A. *Astrophys. J. Lett.* **2014**, *795*, L3, [[CrossRef](#)]
74. Bartoli, B.; Bernardini, P.; Bi, X.J.; Branchini, P.; Budano, A.; Camarri, P.; Cao, Z.; Cardarelli, R.; Catalanotti, S.; Chen, S.Z.; et al. Search for GeV Gamma-Ray Bursts with the ARGO-YBJ Detector: Summary of Eight Years of Observations. *Astrophys. J.* **2014**, *794*, 82, [[CrossRef](#)]
75. Blanch, O.; Gaug, M.; Noda, K.; Berti, A.; Moretti, E.; Miceli, D.; Gliwny, P.; Ubach, S.; Schleicher, B.; Cerruti, M.; et al. MAGIC observations of GRB 201015A: hint of very high energy gamma-ray signal. *GRB Coord. Netw.* **2020**, 28659, 1.
76. MAGIC Collaboration. Observation of inverse Compton emission from a long γ -ray burst. *Nature* **2019**, *575*, 459–463. [[CrossRef](#)]
77. Blanch, O.; Longo, F.; Berti, A.; Fukami, S.; Suda, Y.; Loporchio, S.; Micanovic, S.; Green, J.G.; Pinter, V.; Takahashi, M.; et al. GRB 201216C: MAGIC detection in very high energy gamma rays. *GRB Coord. Netw.* **2020**, 29075, 1.
78. Beardmore, A.P.; Gropp, J.D.; Kennea, J.A.; Klingler, N.J.; Laha, S.; Lien, A.Y.; Moss, M.J.; Page, K.L.; Palmer, D.M.; Tohuvavohu, A.; et al. GRB 201216C: Swift detection of a burst. *GRB Coord. Netw.* **2020**, 29061, 1.
79. Vielfaure, J.B.; Izzo, L.; Xu, D.; Vergani, S.D.; Malesani, D.B.; de Ugarte Postigo, A.; D'Elia, V.; Fynbo, J.P.U.; Kann, D.A.; Leván, A.J.; et al. GRB 201216C: VLT X-shooter spectroscopy and potential high redshift of a VHE-emitting GRB. *GRB Coord. Netw.* **2020**, 29077, 1.
80. Fukami, S.; Berti, A.; Loporchio, S.; Suda, Y.; Nava, L.; Noda, K.; Bošnjak, V.; Asano, K.; Longo, F.; Acciari, V.A.; et al. Very-high-energy gamma-ray emission from GRB 201216C detected by MAGIC. *PoS* **2021**, *ICRC2021*, 788. [[CrossRef](#)]
81. Fermi GBM Team. GRB 190829A: Fermi GBM Final Real-time Localization. *GRB Coord. Netw.* **2019**, 25551, 1.
82. Dichiaro, S.; Bernardini, M.G.; Burrows, D.N.; D'Avanzo, P.; Gronwall, C.; Gropp, J.D.; Kennea, J.A.; Klingler, N.J.; Krimm, H.A.; Kuin, N.P.M.; et al. GRB 190829A: Swift detection of a burst consistent with a galaxy at $z=0.08$. *GRB Coord. Netw.* **2019**, 25552, 1.
83. Hu, Y.D.; Castro-Tirado, A.J.; Kumar, A.; Gupta, R.; Valeev, A.F.; Pandey, S.B.; Kann, D.A.; Castellón, A.; Agudo, I.; Aryan, A.; et al. 10.4 m GTC observations of the nearby VHE-detected GRB 190829A/SN 2019oyw. *Astron. Astrophys.* **2021**, *646*, A50, [[CrossRef](#)]
84. Zhang, B.T.; Murase, K.; Veres, P.; Mészáros, P. External Inverse-Compton Emission from Low-luminosity Gamma-Ray Bursts: Application to GRB 190829A. *Astrophys. J.* **2021**, *920*, 55, [[CrossRef](#)]
85. Zhang, L.L.; Ren, J.; Huang, X.L.; Liang, Y.F.; Lin, D.B.; Liang, E.W. Nearby SN-associated GRB 190829A: Environment, Jet Structure, and VHE Gamma-Ray Afterglows. *Astrophys. J.* **2021**, *917*, 95, [[CrossRef](#)]
86. Salafia, O.S.; Ravasio, M.E.; Yang, J.; An, T.; Orienti, M.; Ghirlanda, G.; Nava, L.; Giroletti, M.; Mohan, P.; Spinelli, R.; et al. Multi-wavelength view of the close-by GRB~190829A sheds light on gamma-ray burst physics. *arXiv* **2021**, arXiv:2106.07169.
87. Roberts, O.J.; Meegan, C. GRB 180720B: Fermi GBM observation. *GRB Coord. Netw.* **2018**, 22981, 1.
88. Evans, P.A.; Breeveld, A.A.; Deich, A.; Gropp, J.D.; Kennea, J.A.; Krimm, H.A.; Lien, A.Y.; Marshall, F.E.; Page, K.L.; Siegel, M.H.; et al. GRB 180620B: Swift detection of a burst with an optical counterpart. *GRB Coord. Netw.* **2018**, 22807, 1.
89. Bissaldi, E.; Racusin, J.L. GRB 180720B : Fermi-LAT detection. *GRB Coord. Netw.* **2018**, 22980, 1.
90. Suda, Y.; Artero, M.; Asano, K.; Berti, A.; Nava, L.; Noda, K.; Terauchi, K.; Acciari, V.A.; Ansoldi, S.; Antonelli, L.A.; et al. Observation of a relatively low luminosity long duration GRB 201015A by the MAGIC telescopes. *PoS* **2021**, *ICRC2021*, 797. [[CrossRef](#)]
91. Ghirlanda, G.; Nappo, F.; Ghisellini, G.; Melandri, A.; Marcarini, G.; Nava, L.; Salafia, O.S.; Campana, S.; Salvaterra, R. Bulk Lorentz factors of gamma-ray bursts. *Astron. Astrophys.* **2018**, *609*, A112, [[CrossRef](#)]
92. Zhang, S.; Shao, L.; Zhang, B.B.; Zou, J.H.; Sun, H.Y.; Yao, Y.j.; Li, L.L. A Tight Three-parameter Correlation and Related Classification on Gamma-Ray Bursts. *Astrophys. J.* **2022**, *926*, 170, [[CrossRef](#)]
93. Li, Y.; Zhang, B.; Lü, H.J. A COMPARATIVE STUDY OF LONG AND SHORT GRBS. I. OVERLAPPING PROPERTIES. *Astrophys. J. Suppl. Ser.* **2016**, *227*, 7. [[CrossRef](#)]
94. Wood, J. Results from the first one and a half years of the HAWC GRB program. *arXiv* **2018**, arXiv:1801.01437.
95. Carosi, A.; Ashkar, H.; Berti, A.; Bordas, P.; de Bony Lavergne, M.; Donini, A.; Dalchenko, M.; Fiasson, A.; Foffano, L.; Fukami, S.; et al. First follow-up of transient events with the CTA Large Size Telescope prototype. In Proceedings of the 37th International Cosmic Ray Conference, Berlin, Germany, 12–23 July 2021.
96. Acciari, V.A.; Ansoldi, S.; Antonelli, L.A.; Arbet Engels, A.; Asano, K.; Baack, D.; Babić, A.; Baquero, A.; Barres de Almeida, U.; Barrio, J.A.; et al. MAGIC Observations of the Nearby Short Gamma-Ray Burst GRB 160821B. *Astrophys. J.* **2021**, *908*, 90, [[CrossRef](#)]
97. Acciari, V.A.; Ansoldi, S.; Antonelli, L.A.; Arbet Engels, A.; Baack, D.; Babić, A.; Banerjee, B.; Barres de Almeida, U.; Barrio, J.A.; Becerra González, J.; et al. Bounds on Lorentz Invariance Violation from MAGIC Observation of GRB 190114C. *Phys. Rev. Lett.* **2020**, *125*, 021301, [[CrossRef](#)]
98. Abdalla, H.; Abe, H.; Acero, F.; Acharyya, A.; Adam, R.; Agudo, I.; Aguirre-Santaella, A.; Alfaro, R.; Alfaro, J.; Alispach, C.; et al. Sensitivity of the Cherenkov Telescope Array for probing cosmology and fundamental physics with gamma-ray propagation. *J. Cosmol. Astropart. Phys.* **2021**, *2021*, 048, [[CrossRef](#)]

99. Carosi, A.; López-Oramas, A.; Longo, F. The Cherenkov Telescope Array transient and multi-messenger program. In Proceedings of the 37th International Cosmic Ray Conference, Berlin, Germany, 12–23 July 2021.
100. Inoue, S.; Granot, J.; O'Brien, P.T.; Asano, K.; Bouvier, A.; Carosi, A.; Connaughton, V.; Garczarczyk, M.; Gilmore, R.; Hinton, J.; et al. Gamma-ray burst science in the era of the Cherenkov Telescope Array. *Astropart. Phys.* **2013**, *43*, 252–275. [[CrossRef](#)]
101. Bernardini, M.G.; Bissaldi, E.; Bosnjak, Z.; Carosi, A.; D'Avanzo, P.; Di Girolamo, T.; Inoue, S.; Gasparetto, T.; Ghirlanda, F.; Longo, F.; et al. POSyTIVE-a GRB population study for the Cherenkov Telescope Array. In Proceedings of the 36th International Cosmic Ray Conference (ICRC2019), Madison, WI, USA, 24 July–1 August 2019; International Cosmic Ray Conference; Volume 36, p. 598.
102. Amati, L.; Frontera, F.; Tavani, M.; in't Zand, J.J.M.; Antonelli, A.; Costa, E.; Feroci, M.; Guidorzi, C.; Heise, J.; Masetti, N.; et al. Intrinsic spectra and energetics of BeppoSAX Gamma-Ray Bursts with known redshifts. *Astron. Astrophys.* **2002**, *390*, 81–89. [[CrossRef](#)]
103. Cortina, J.; Project, C.L. Status of the Large Size Telescopes of the Cherenkov Telescope Array. In Proceedings of the 36th International Cosmic Ray Conference (ICRC2019), Madison, WI, USA, 24 July–1 August 2019; International Cosmic Ray Conference; Volume 36, p. 653.
104. Scuderi, S. *The ASTRI Mini-Array at the Teide Observatory*; Society of Photo-Optical Instrumentation Engineers (SPIE) Conference Series; Society of Photo-Optical Instrumentation Engineers: Bellingham, WA, USA, 2021; Volume 11822, p. 1182202. [[CrossRef](#)]
105. Stamerra, A.; Saturni, F.G.; Green, J.; Nava, L.; Lucarelli, F.; Antonelli, L. TeV Transients with the ASTRI Mini-Array: A case study with GRB 190114C. In Proceedings of the 37th International Cosmic Ray Conference (ICRC2021), Berlin, Germany, 12–23 July 2021; International Cosmic Ray Conference; Volume 395, p. 890.